Pergamon

Geochimica et Cosmochimica Acta, Vol. 66, No. 21, pp. 3769–3788, 2002

0016-7037/02 $22.00 + .00

PII S0016-7037(02)00887-6

Experimental and theoretical study of pressure effects on hydrogen isotope fractionation in the system brucite-water at elevated temperatures

JUSKE HORITA,[1,*] DAVID R. COLE,[1] VENIAMIN B. POLYAKOV,[2] and THOMAS DRIESNER[3]

[1]Chemical Sciences Division, Oak Ridge National Laboratory, Oak Ridge, TN 37831-6110, USA
[2]V. I. Vernadsky Institute of Geochemistry and Analytical Chemistry, Russian Academy of Science, Moscow B-334, Russia
[3]Isotope Geochemistry and Mineral Resources, ETH Zentrum, CH-8092 Zurich, Switzerland

(*Received June* 25, 2001; *accepted in revised form March* 13, 2002)

Abstract—A detailed, systematic experimental and theoretical study was conducted to investigate the effect of pressure on equilibrium D/H fractionation between brucite ($Mg(OH)_2$) and water at temperatures from 200 to 600°C and pressures up to 800 MPa. A fine-grained brucite was isotopically exchanged with excess amounts of water, and equilibrium D/H fractionation factors were calculated by means of the partial isotope exchange method. Our experiments unambiguously demonstrated that the D/H fractionation factor between brucite and water increased by 4.4 to 12.4‰ with increasing pressure to 300 or 800 MPa at all the temperatures investigated. The observed increases are linear with the density of water under experimental conditions. We calculated the pressure effects on the reduced partition function ratios (β-factor) of brucite (300–800 K and $P \leq 800$ MPa) and water (400–600°C and $P \leq 100$ MPa), employing a statistical-mechanical method similar to that developed by Kieffer (1982) and a simple thermodynamic method based on the molar volumes of normal and heavy waters, respectively. Our theoretical calculations showed that the reduced partition function ratio of brucite increases linearly with pressure at a given temperature (as much as 12.6‰ at 300 K and 800 MPa). The magnitude of the pressure effects rapidly decreases with increasing temperature. On the other hand, the β-factor of water decreases 4 to 5‰ with increasing pressure to 100 MPa at 400 to 600°C. Overall D/H isotope pressure effects combined from the separate calculations on brucite and water are in excellent agreement with the experimental results under the same temperature-pressure range. Our calculations also suggest that under the current experimental conditions, the magnitude of the isotope pressure effects is much larger on water than brucite. Thus, the observed pressure effects on D/H fractionation are common to other systems involving water. It is very likely that under some geologic conditions, pressure is an important variable in controlling D/H partitioning. *Copyright © 2002 Elsevier Science Ltd*

1. INTRODUCTION

Temperature and pressure are the two most important variables that determine the thermodynamics of earth materials and equilibrium distributions of chemical elements among them. Despite a very wide range of pressure encountered in nature, ranging from near-vacuum (≤0.1 KPa) at interplanetary conditions to ultrahigh pressures (≥10 GPa) at great depths in planets, it has been commonly assumed in stable isotope geochemistry and cosmochemistry that equilibrium partitioning of the isotopes of light elements (hydrogen, oxygen, carbon, sulfur, etc.) among different phases and chemical species (minerals, waters, gases, dissolved species, etc.) depends largely on temperature, but not on pressure. This unique feature of isotopic fractionation, known as isotope geothermometry with minimum pressure corrections, if any, distinguishes isotopic techniques from other geochemical methods.

The fundamental premise that isotopic partitioning is largely pressure-independent originates from the assumptions that isotopes of a given element have the same electronic configuration (the Born-Oppenheimer approximation) and that the harmonic approximation can be used in the calculation of isotope fractionation factors. Although justifiable to a first approximation, these assumptions are not exactly correct. Since the birth of isotope geochemistry in the 1950s, this fundamental issue of the pressure-independence of isotopic partitioning has been addressed many times, both experimentally and theoretically. However, our current knowledge of pressure effects on isotopic partitioning in nature is still very limited. With a renewed interest during the last decade, we initiated a systematic experimental and theoretical study to investigate the isotope pressure effects under geologically relevant conditions. A first set of experimental results on the isotope pressure effects of the brucite-water system at 380°C has been presented by Horita et al. (1999). In this study, we extended our systematic experiments to a broad temperature-pressure range (200–600°C and pressures up to 300 MPa). We also conducted a rigorous theoretical study of the isotope pressure effects in the brucite-water system to compare these results with our experimental results and to gain insight into the cause of the isotope pressure effects in the system hydrous mineral-water system in general.

2. PREVIOUS STUDIES

Hoering (1961) was the first to examine experimentally the pressure effect on oxygen isotope partitioning between HCO_3^- (*aq*) and liquid water at 43.5°C and at 0.1 and 400 MPa but did not observe any difference in the fractionation factor beyond analytical errors of 0.2‰. Clayton et al. (1975) carried out a systematic study of calcite-water fractionation at 500°C and 0.1 to 2 GPa and at 700°C and 50 and 100 MPa but observed no measurable pressure effects. Studies conducted by the Chicago

* Author to whom correspondence should be addressed (horitaj@ornl.gov).

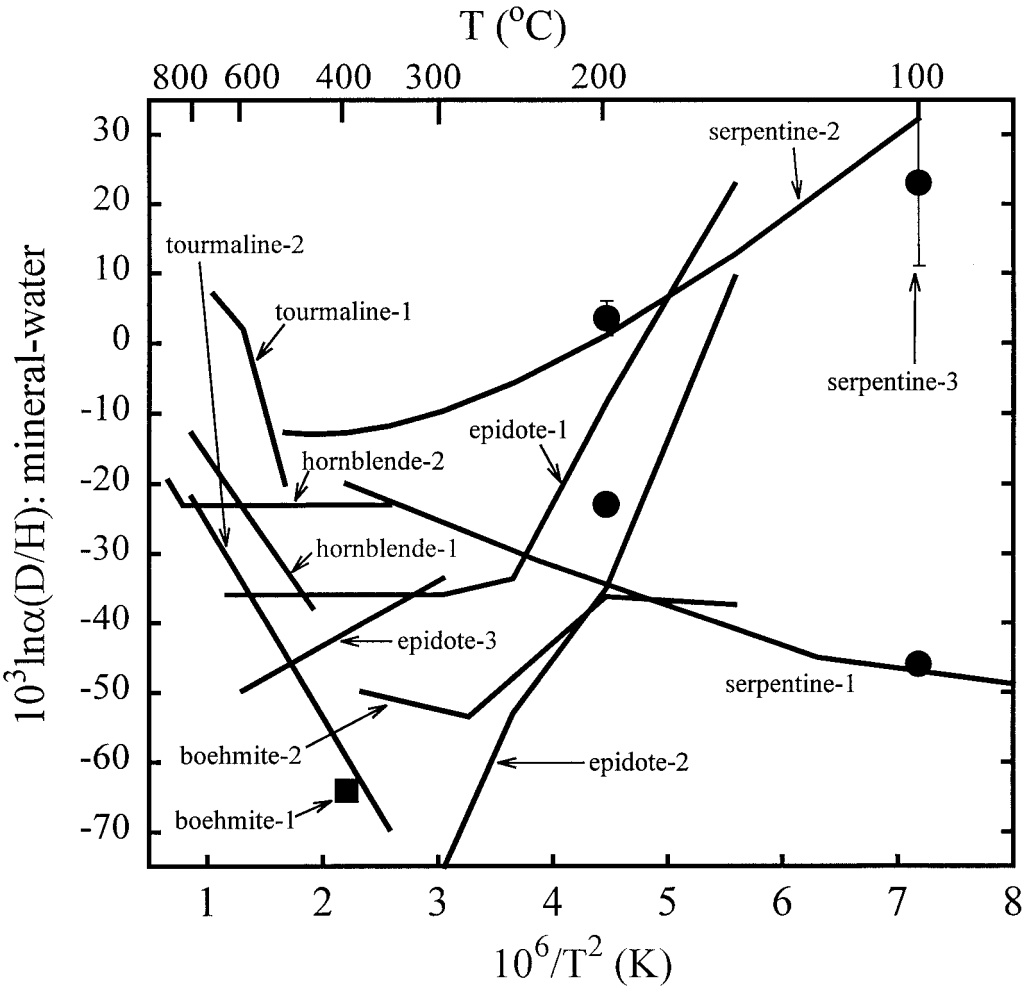

Fig. 1. Literature data on D/H isotope fractionation of several hydrous minerals-water systems: serpentine-1 (Wenner and Taylor, 1973), serpentine-2 (Sakai and Tsutsumi, 1978), and serpentine-3 (all solid circles) (Mineev and Grinenko, 1996); boehmite-1 (Suzuoki and Epstein, 1976) and boehmite-2 (Graham et al., 1980); epidote-1 (Graham et al., 1980), epidote-2 (Vennemann and O'Neil, 1996), and epidote-3 (Chacko et al., 1999); hornblende-1 (Suzuoki and Epstein, 1976) and hornblende-2 (Graham et al., 1984); tourmaline-1 (Blamart et al., 1989) and tourmaline-2 (Guo and Qian, 1997).

group on quartz-water at 700°C and 0.2 to 1.5 GPa, at 400°C and 0.2 to 2.2 GPa, and at 600°C and 0.6 to 2.0 GPa (Matsuhisa et al., 1979; Matthews et al., 1983a); wollastonite-water at 600°C and 0.9 to 2.0 GPa (Matthews et al., 1983a); and albite-water at 500°C and 0.2 to 1.5 GPa (Matthews et al., 1983b) also yielded no discernible pressure effects on $^{18}O/^{16}O$ fractionation. In addition, several mineral-water systems, notably calcite, quartz, and albite, have been revisited for their $^{18}O/^{16}O$ fractionation by the Chicago group. Clayton et al., (1989), and later Rosenbaum (1997), found gross discrepancies (on the order of 2‰ at 350–700°C) in mineral-water oxygen isotope fractionation between those experimentally determined at high water pressures and the others obtained from calculated reduced partition function ratios of minerals and water (assuming isolated water molecules). These investigators argued that the observed difference in partition function ratios of water (calculated as isolated water molecules vs. experimentally derived at high pressures) is due to non-ideal behavior of real water at high temperatures and pressures. However, a recent systematic experimental study by Hu and Clayton (2002) strongly suggests that dissolved minerals in water at elevated temperatures and pressures are the cause of these large discrepancies. It is largely based on the work of the Chicago group, especially of Clayton et al. (1975), that pressure has been considered a very minor variable, if any, on oxygen isotope fractionation.

Hydrogen isotope fractionation of several hydrous mineral-water systems has been studied by different investigators at somewhat different experimental conditions (Fig. 1). The isotope pressure effects were often invoked to explain large discrepancies of D/H partitioning observed among studies conducted at different pressures on the same mineral-water systems. The system epidote-water was studied by Graham et al. (1980) at 200 to 650°C and 200 to 400 MPa, by Vennemann and O'Neil (1996) at 150 to 400°C with low pressure H_2 gas as an exchange medium, and by Chacko et al., (1999) at 300 to 600°C and 120 to 230 MPa. Vennemann and O'Neil (1996) obtained epidote-water D/H fractionation factors by combining

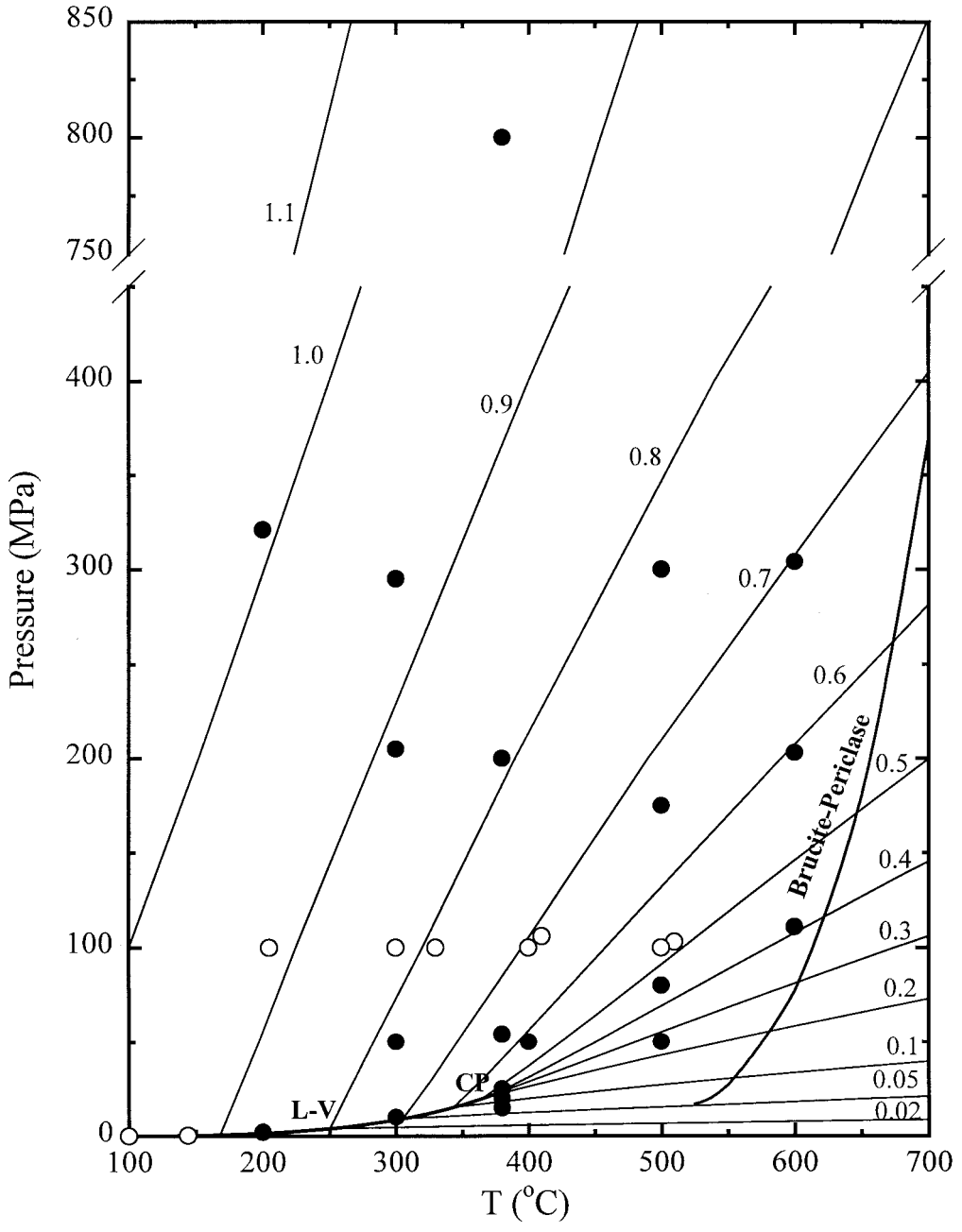

Fig. 2. Experimental P-T matrix of brucite-water D/H fractionation with the isochors of water (g/cm^3): closed circle, this study; open circle, Satake and Matsuo (1984). L-V: liquid-vapor boundary; CP: critical point.

their experimental results of epidote-H_2 fractionation with experimental and theoretical results of water-H_2 in the literature. Their results are up to 40‰ smaller than direct experimental measurements by Graham et al. (1980) and Chacko et al. (1999) (Fig. 1). Large (up to 60‰) differences exist also in D/H fractionation between serpentine-water obtained empirically by Wenner and Taylor (1973) and experimentally by Sakai and Tsutsumi (1978). Experimental results of serpentine-water at 100°C and 0.1 and 250 MPa and at 200°C and 0.1 and 100 MPa by Mineev and Grinenko (1996) suggested possible pressure effects for this discrepancy (Fig. 1), but details of their experimental results are not documented. Tourmaline-water D/H fractionation was determined by Blamart et al. (1989) and Guo and Qian (1997). The former results at 300 MPa are 20 to 35‰ higher than the latter at 500 to 600°C and 15 to 25 MPa. Hornblende-water D/H fractionation studied by Suzuoki and Epstein (1976) and Graham et al. (1984) show different temperature dependencies with differences up to 15‰: The former study was conducted at 100 MPa and the latter at 200 to 800 MPa. Although pressure differences among these experimental studies may explain discrepancies in D/H fractionation factors of these hydrous mineral-water systems, no detailed systematic study has been conducted for investigating the effect of pressure on D/H isotope fractionation.

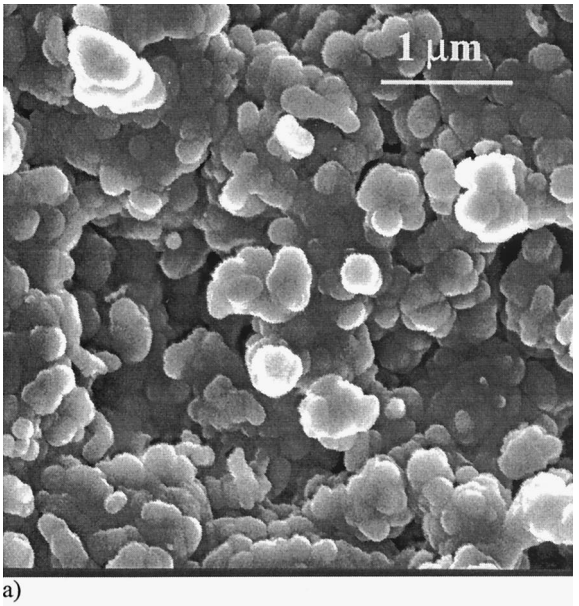

a)

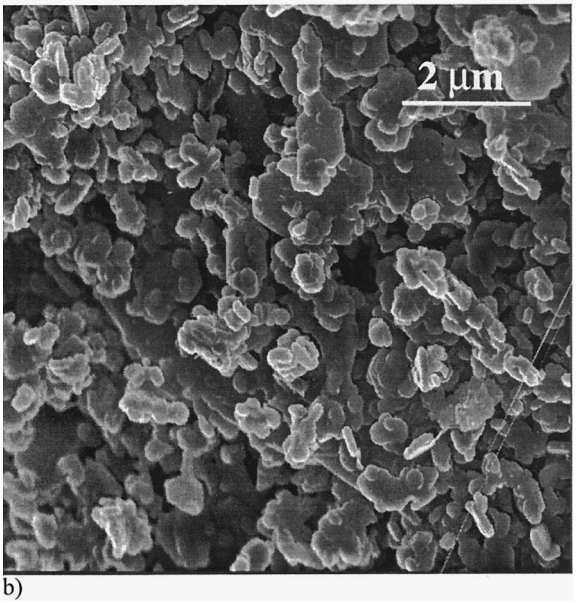

b)

Fig. 3. SEM photomicrographs of brucite. (a) starting material; (b) after run at 300°C and 10.7 MPa for 2205 h.

Several investigators calculated the pressure effect on equilibrium oxygen and hydrogen isotope fractionation, mostly for minerals (Joy and Libby, 1960; Clayton et al., 1975; Hamann et al., 1984; Schmid et al., 1989; Heybey and Wand, 1989; Vörtler and Heybey, 1989; Sharp et al., 1992; Polyakov and Kharlashina, 1994; Gillet et al., 1996; Polyakov, 1998). However, the sign and magnitude of pressure-induced changes in the reduced partition function ratios of minerals vary widely among the different studies reported in the literature. It is argued that since changes in the molar volume of a phase caused by isotopic substitution are largely canceled out by a similar change in another coexisting phase, an overall fractionation factor between the two phases would not be affected significantly by pressure change. This could well be true for a mineral-mineral pair, but may not be the case for a mineral-fluid pair because of large pressure-induced changes in the molar volume and structure of fluids. Polyakov and Kharlashina (1994) calculated, based on thermodynamics, that the pressure effect on the D/H reduced partition function ratio of pure water is much larger than that of the mineral brucite and that the sign of the two pressure effects are opposite to each other. More recently, Driesner (1997) used pressure-induced red-shifts of O-H stretching frequencies of water at high temperatures reported by Frantz et al. (1993) to calculate changes by as much as 20‰ in the reduced partition function ratios of pure water from 22 to 200 MPa near the critical temperature of water (374°C). Driesner (1997) argued that some discrepancies in published experimental D/H fractionation factors between hydrous minerals and water discussed above, particularly of epidote-water between Graham et al. (1980) and Vennemann and O'Neil (1996), could be ascribed to the pressure difference of the experiments. The magnitude of the calculated pressure effects on D/H isotope partitioning in water and the discrepancies in mineral-water D/H partitioning in the literature are too large to be ignored.

Table 1. D/H ratios of starting materials.

	δD (‰)
Starting brucite	
Brucite-A	−84.07 ± 0.38 (n = 4)
Water	
W-1	−45.04 ± 0.53 (n = 2)
W-4	−291.56 ± 0.37 (n = 4)
W-5	197.37 ± 0.10 (n = 2)
W-6	103.85 ± 0.22 (n = 2)
W-7	24.36 ± 0.07 (n = 3)
W-8	−104.91 ± 0.73 (n = 3)

Errors are in 1 σ.

3. THEORETICAL BACKGROUND OF ISOTOPE PRESSURE EFFECTS

An equilibrium isotope fractionation factor between two compounds A and B ($\alpha_{A\text{-}B}$) is defined as:

$$\alpha_{A-B} = \frac{\beta_A}{\beta_B} = \frac{(X^*/X)_A}{(X^*/X)_B} \tag{1}$$

where X is an element of interest in the compound and the asterisk denotes heavy isotopes. The β-factor has been previously defined by Varshavsky and Vaisberg (1957), Richet et al. (1977), and Galimov (1985):

$$\beta \equiv \left(\frac{(Q^*/Q)_{quant}}{(Q^*/Q)_{class}}\right)^{1/n} = \left[\left(\frac{s^*}{s}\right) f\right]^{1/n} = \left[\left(\frac{s^*}{s}\right) \prod_i^n \left(\frac{m_i}{m_i^*}\right)^{3/2} \left(\frac{Q^*}{Q}\right)_{quant}\right]^{1/n} \tag{2}$$

where Q is the partition function and the subscripts *quant* and

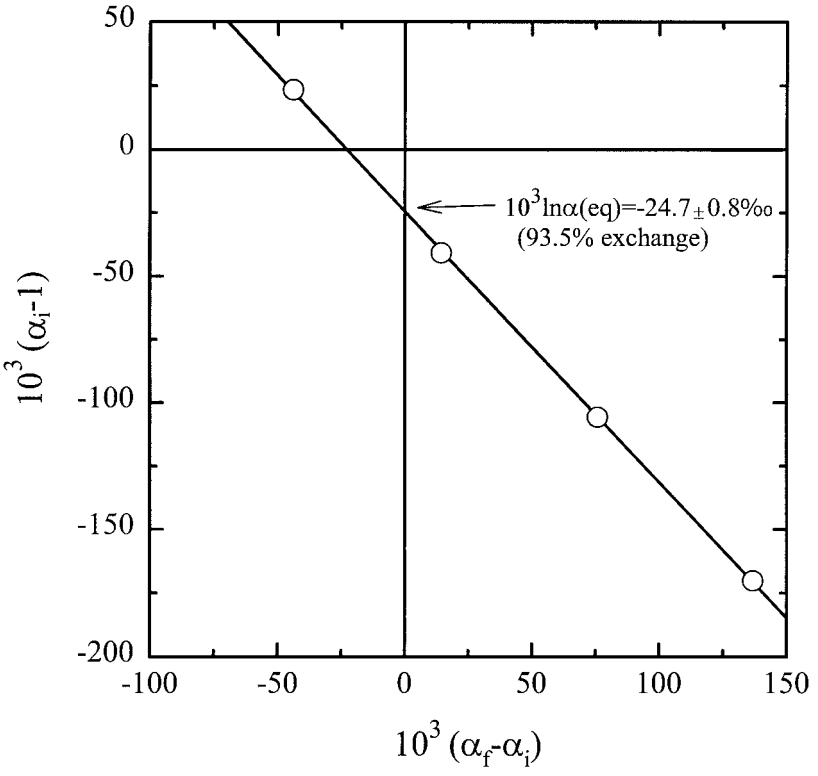

Fig. 4. Example of a fit of the Northrop and Clayton (1966) partial exchange method: Run I at 380°C and 200 MPa (Table 2).

class refer to values calculated according to quantum and classical mechanics, respectively. The *m* is the atomic weight of the element *X*, *i* refers to its positions within a compound, and *n* is the number of isotopes to be exchanged. The *s* is the symmetry number, which is the same for homogeneous isotopomers of a given compound (e.g., H_2O and D_2O). The *f* is the reduced partition function ratio defined by Bigeleisen and Mayer (1947) and Urey (1947). Thus, the β-factor is equivalent to the reduced partition function ratio for an exchange reaction of one isotope.

The effect of pressure on isotopic partitioning is defined as

$$\Gamma_P = \frac{\alpha_{A-B,P}}{\alpha_{A-B,P(ref)}} \tag{3}$$

where *P(ref)* is a reference pressure. Then,

$$10^3 \ln \Gamma_P = 10^3 \ln \alpha_{A-B,P} - 10^3 \ln \alpha_{A-B,P(ref)} \tag{4}$$

$$= 10^3(\ln \beta_{A,P} - \ln \beta_{B,P}) - 10^3(\ln \beta_{A,P(ref)} - \ln \beta_{B,P(ref)}) \tag{5}$$

$$= 10^3 \ln\left[\frac{\beta_{A,P}}{\beta_{A,P(ref)}}\right] - 10^3 \ln\left[\frac{\beta_{B,P}}{\beta_{B,P(ref)}}\right] = 10^3 (\Delta \ln \beta_A - \Delta \ln \beta_B) \tag{6}$$

If the pressure effect on minerals and other coexisting phases is negligible in systems involving aqueous fluids ($\alpha_{\text{A-water}}$), the isotope pressure effect is derived solely from the properties of aqueous solutions:

$$10^3 \ln \Gamma_p = -10^3 \ln\left[\frac{\beta_{Pure\text{-}water,P}}{\beta_{Pure\text{-}water,P(ref)}}\right] = -10^3 \Delta \ln \beta_{Pure\text{-}water} \tag{7}$$

From laboratory experiments, only overall pressure effects on isotopic partitioning between two substances can be determined.

The conventional wisdom that pressure has little affect on isotope partitioning can be justified if we assume (a) that the intermolecular forces between pairs of like-molecules (e.g., H_2O-H_2O) and between pairs of unlike molecules (e.g., H_2O-D_2O) are the same and (b) that different isotopic molecules (e.g., H_2O, D_2O, $H_2{}^{18}O$) of the same compounds (isotopomers) have the same molar volume. The former assumption (a) is, to a large extent, rationalized within the Born-Oppenheimer approximation, but the latter (b) is not the case. Theoretical analysis demonstrated that pressure effects on mixtures of isotopic molecules are closely connected to the difference between the molar volumes of different isotopic molecules, i.e., molar volume isotope effects (MVIE), which in turn are well understood in terms of isotope effects on vibrational amplitude (for review, see Jancsó et al., 1993).

The β-factor in Eqn. 2 can be expressed in terms of the Gibbs free energy (*G*) (e.g., Polyakov, 1998):

$$\ln \beta = -\frac{G^* - G}{nRT} + \frac{3}{2} \ln \frac{m}{m^*} \tag{8}$$

where *R* is the universal gas constant and *T* is the absolute

Table 2. Experimental results of pressure effects on D/H partitioning between brucite and water.

Sample No	Water type	Water (mg)	Brucite (mg)	δD (‰) Brucite(f)	Water(f)calc	Water(f)meas	diff[a]	$10^3(\alpha_i-1)$	$10^3(\alpha_f-\alpha_i)$	$10^3 \ln\alpha_{eq}$[b]	F(%)[c]
200.3°C/2.1 MPa (4460h)											
Brucite-1X	W-1	500.10	100.48	−79.14	−45.15			−37.57	1.97	−35.85 ± 0.72	91.7
Brucite-5X	W-4	499.28	103.36	−283.92	−278.58			297.33	−304.73		
Brucite-9X	W-5	500.95	101.26	123.68	184.59			−232.42	180.99		
Brucite-13X	W-6	506.54	101.23	45.22	96.07			−167.39	121.00		
200°C/321 MPa (376.9h)											
6M	W-1	120.65	21.04	−73.88	−45.58			−40.87	11.23	−28.70 ± 0.87	89.0
6N	W-6	122.21	21.08	49.16	96.75	96.49	−0.26	−170.24	126.85		
6O	W-7	122.16	21.28	−17.50	20.77	19.27	−1.5	−105.85	68.35		
6P	W-8	119.84	21.14	−122.91	−102.79	−105.24	−2.44	23.283	−45.710		
300°C/10.7 MPa (2205h)											
Brucite-1	W-1	519.68	112.75	−77.68	−45.25			−37.57	3.61	−31.84 ± 1.55	92.2
Brucite-5	W-4	507.09	109.60	−281.55	−278.16			297.33	−302.03		
Brucite-9	W-5	496.91	100.55	131.75	184.07			−232.41	188.22		
Brucite-13	W-6	534.75	109.95	47.84	95.68			−167.39	123.72		
300°C/50 MPa (1516.7h)											
I	W-1	108.94	20.39	−73.49	−45.65	−46.59	−0.94	−40.87	11.70	−29.26 ± 0.81	97.8
II	W-6	109.48	20.37	60.74	95.53	95.42	−0.11	−170.24	138.49		
III	W-7	107.83	20.32	−11.15	20.11	19.05	−1.06	−105.85	75.20		
IV	W-8	108.97	20.50	−127.19	−102.40	−105.16	−2.76	23.28	−50.89		
300°C/200 MPa (1540.4h)											
V	W-1	201.06	20.40	−69.79	−45.48	−45.71	−0.22	−40.87	15.40	−26.96 ± 0.82	97.4
VI	W-6	198.64	20.70	65.66	99.03	99.75	0.72	−170.24	139.88		
VII	W-7	200.44	20.58	−7.93	21.94	20.59	−1.35	−105.85	76.62		
VIII	W-8	200.7	20.46	−126.97	−103.56	−106.46	−2.91	23.28	−49.39		
300°C/300 MPa (100.7h)											
IX	W-1	199.49	20.58	−69.01	−45.52	−45.85	−0.33	−40.87	16.26	−26.18 ± 1.62	92.8
X	W-6	201.14	20.31	57.92	99.42	99.73	0.31	−170.24	132.49		
XI	W-7	201.47	20.48	−9.11	22.00	20.62	−1.39	−105.85	75.41		
XII	W-8	197.61	20.51	−125.29	−103.59	−106.28	−2.69	23.28	−47.50		
380°C/15 MPa (1751h)											
28	W-8	38.1	17.8	−122.59	−99.35	−101.9	−2.55	23.28	−49.09	−31.96 ± 0.94	90.8
29	W-1	48.4	15.5	−77.65	−45.67			−40.87	7.37		
30	W-7	37.8	20.5	−23.98	14.29			−105.85	68.12		
380°C/20 MPa (1751h)											
2	W-8	102.4	19.1	−128.12	−102.37	−105.58	−3.21	23.28	−51.96	−31.44 ± 1.10	93.9
5	W-1	80.4	14.0	−74.97	−45.53	−46.35	−0.83	−40.87	10.03		
8	W-7	97.0	16.8	−13.90	20.60	18.86	−1.74	−105.85	72.04		
11	W-6	97.2	19.5	50.77	95.50			−170.24	129.41		
380°C/25 MPa (1751h)											
1	W-8	272.3	16.80	−128.34	−104.07	−108.02	−3.96	23.28	−50.38	−28.07 ± 0.81	98.2
4	W-1	206.1	18.80	−71.76	−45.38	−46.67	−1.28	−40.87	13.24		
7	W-7	175.7	15.10	−6.98	22.31	20.85	−1.46	−105.85	77.20		
10	W-6	175.4	15.40	66.11	99.78	98.52	−1.26	−170.24	139.63		
380°C/54 MPa (1299h)											
I	W-1	50.86	12.38	−71.07	−46.01	−47.23	−1.21	−40.87	14.61	−25.59 ± 0.85	94.4
II	W-6	50.53	12.53	56.98	93.05	92.66	−0.39	−170.24	137.24		
III	W-7	49.66	12.60	−12.12	18.72	16.85	−1.86	−105.85	75.58		
IV	W-8	50.27	12.57	−122.00	−101.98	−102.24	−0.26	23.28	−45.57		
380°C/200 MPa (864h)											
I	W-8	129.95	25.92	−121.08	−102.63			23.28	−43.85	−24.70 ± 0.86	93.5
II	W-7	132.25	25.76	−10.60	19.94			−105.85	75.91		
III	W-6	129.73	25.89	58.40	95.07			−170.24	136.76		
IV	W-1	129.4	26.06	−71.08	−45.84			−40.87	14.43		
380°C/800 MPa (283.5h)											
5	W-8	24.58	9.61	−115.89	−101.07	−104.01	−2.94	23.28	−39.77	−19.52 ± 2.48	93.4
6	W-1	25.43	9.80	−65.03	−47.30	−46.11	1.19	−40.87	22.27		
7	W-7	26.06	10.01	−13.79	16.02	11.88	−4.13	−105.85	76.51		
8	W-6	26.10	10.12	57.36	86.91	84.27	−2.64	−170.24	143.06		
400°C/51.5 MPa (1103h)											
Brucite-85	W-4	350.25	70.03	−284.97	−278.9			297.33	−305.68	−26.04 ± 1.43	97.1
Brucite-81	W-1	349.89	70.63	−70.34	−45.69			−37.57	11.75		
Brucite-93	W-6	242.87	49.83	61.37	94.84			−167.39	136.82		
Brucite-89	W-5	357.93	71.72	146.25	183.31			−232.42	201.10		
500°C/52 MPa (2659.5h)											
B9	W-1	52.33	13.46	−70.05	−46.15			−40.87	15.81	−27.01 ± 2.13	96.0

(continued on next page)

Table 2. (continued).

Sample No	Water type	Water (mg)	Brucite (mg)	δD (‰) Brucite(f)	Water(f)calc	Water(f)meas	diff[a]	$10^3(\alpha_i-1)$	$10^3(\alpha_f-\alpha_i)$	$10^3 In\alpha_{eq}$[b]	F(%)[c]
B10	W-6	51.92	13.51	59.08	92.35	89.13	−3.21	−170.24	139.79		
B11	W-7	52.15	13.76	−15.58	18.77	16.24	−2.53	−105.85	72.12		
B12	W-8	52.42	13.42	−123.99	−101.75	−102.68	−0.93	23.28	−48.03		
496°C/81.1 MPa (670h)											
Brucite-49	W-1	347.63	69.82	−69.75	−45.73			−37.57	12.40	−24.77 ± 0.70	95.3
Brucite-54	W-4	362.66	69.86	−286.28	−279.34			297.33	−306.97		
Brucite-57	W-5	354.67	70.34	141.93	183.72			−232.41	197.11		
Brucite-61	W-6	355.97	70.12	62.56	95.12			−167.39	137.65		
500°C/175 MPa (2641.6h)											
B5	W-1	113.24	21.60	−67.35	−46.02	−46.53	−0.51	−40.87	18.51	−21.58 ± 0.86	96.0
B6	W-6	112.73	21.47	65.54	95.05	95.29	0.24	−170.24	143.29		
B7	W-7	112.78	21.89	−5.94	19.67	18.74	−0.93	−105.85	80.73		
B8	W-8	113.71	22.15	−120.04	−102.75	−103.24	−0.50	23.28	−42.56		
500°C/300 MPa (101.1h)											
1	W-1	112.59	21.57	−64.93	−46.17	−46.77	−0.60	−40.87	21.21	−20.27 ± 1.59	93.7
2	W-6	112.78	21.59	64.02	95.10	95.26	0.17	−170.24	141.87		
3	W-7	112.85	21.34	−8.77	19.96	19.01	−0.94	−105.85	77.68		
4	W-8	112.71	21.37	−118.62	−102.89	−103.04	−0.15	23.28	−40.82		
600°C/111 MPa (764.7h)											
6B	W-6	149.85	20.95	69.41	97.23	95.34	−1.88	−170.24	144.89	−24.61 ± 0.99	98.9
6C	W-7	151.04	20.94	−5.677	21.00	18.67	−2.33	−105.85	79.72		
6D	W-8	149.91	20.52	−124.26	−103.21	−106.27	−3.06	23.28	−46.76		
600°C/203 MPa (765.1h)											
6F	W-6	149.79	20.21	69.86	97.44	97.79	0.35	−170.24	145.11	−22.10 ± 1.01	97.8
6G	W-7	149.19	20.20	−3.09	20.97			−105.85	82.28		
6H	W-8	150.74	20.40	−122.07	−103.32	−106.47	−3.15	23.28	−44.20		
600°C/304 MPa (170.7h)											
6I	W-1	122.57	20.83	−65.43	−46.01	−46.92	−0.90	−40.87	20.52	−20.24 ± 0.89	92.8
6J	W-6	122.34	20.71	59.28	96.36	95.96	−0.40	−170.24	136.43		
6K	W-7	122.50	20.97	−2.90	20.06	18.55	−1.51	−105.85	83.34		
6L	W-8	121.01	20.48	−119.99	−103.03	−105.77	−2.73	23.28	−42.18		

[a], diff = δD(water)final, calculated - δD(water)final, measured.
[b], calculated from the Northrop and Clayton (1966) method.
[c], F (fraction of exchange)= $100x(\alpha_f-\alpha_{eq})/(\alpha_i-\alpha_{eq})$.

temperature (K). The differentiation of the β-factor with respect to pressure, using the thermodynamic relation $V = (\partial G/\partial P)_T$, leads to (Clayton et al., 1975; Polyakov, 1998):

$$\left(\frac{\partial \ln \beta}{\partial P}\right)_T = -\frac{\Delta V}{nRT} \tag{9}$$

where V is the molar volume of isotopic species and $\Delta V = V^*-V$ is the molar volume isotope effect (MVIE) at a given temperature and pressure. $V(H_2{}^{18}O)$ is smaller by 0.15% than $V(H_2{}^{16}O)$ at ambient temperature and pressure, i.e., normal MVIE ($\Delta V = V^*-V < 0$). However, $V(D_2O)$ is larger by 0.17% than $V(H_2O)$ at ambient temperature and pressure, i.e., inverse MVIE ($\Delta V = V^*-V > 0$) (Jancsó et al., 1993):

$$V(D_2{}^{16}O) > V(H_2{}^{16}O) > V(H_2{}^{18}O) \tag{10}$$

Thus, $\left(\frac{\partial \ln\beta}{\partial P}\right)_T = -\frac{\Delta V}{nRT} < 0$ for D_2O (and HDO), while $\left(\frac{\partial \ln\beta}{\partial P}\right)_T = -\frac{\Delta V}{nRT} > 0$ for $H_2{}^{18}O$ and most of other compounds. This examination of MVIE suggests that the D/H-reduced partition function ratios for water and coexisting phases (e.g., minerals) decrease and increase with pressure, respectively. Thus, D/H fractionation between coexisting phases and water increases with increasing pressure. On the other hand, it is most likely that the $^{18}O/^{16}O$-reduced partition function ratios for both water and coexisting phases increase with pressure. If the effects on the two phases are similar in magnitude, an $^{18}O/^{16}O$ fractionation between coexisting phases and water does not change measurably with pressure.

4. EXPERIMENTAL STUDY

4.1. Experimental

We chose a brucite [$Mg(OH)_2$]-pure water system to investigate the effect of pressure on equilibrium D/H fractionation represented by the following reaction:

$$½Mg(OH)_2 + ½D_2O \leftrightarrow ½Mg(OD)_2 + ½H_2O \tag{11}$$

and

$$\alpha_{Brucite\text{-}water} = \frac{\beta_{Brucite}}{\beta_{Water}} = \frac{(D/H)_{Brucite}}{(D/H)_{Wat/Water}} \tag{12}$$

Brucite is chemically and structurally a simple mineral stable over a wide pressure-temperature range. Its solubility in water is low (Walter, 1986) and water content is high (stoichiometric value: 30.9%). In addition, several investigators reported ther-

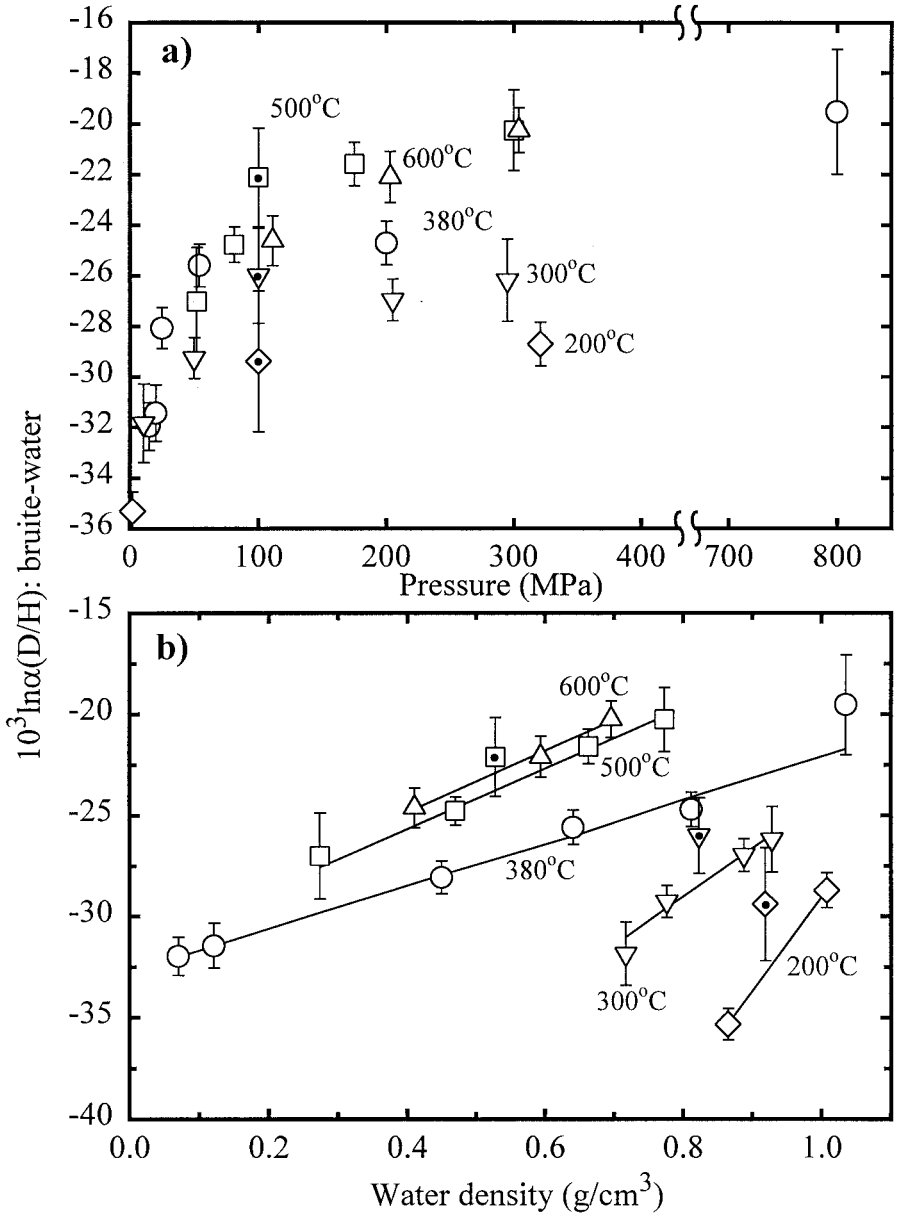

Fig. 5. Experimental results of the pressure effects on brucite-water D/H fractionation factor as a function of (a) pressure and (b) density of water (◇, 200°C; ▽, 300°C; ○, 380°C; □, 500°C; △, 600°C). Dotted symbols from Satake and Matsuo (1984).

modynamic and spectroscopic properties of brucite at very high temperatures and pressures (e.g., Gillet et al., 1996; Bai and Koster van Groos, 1998). These properties make brucite very suitable for the investigation of the isotope pressure effects, both experimental and theoretical.

We conducted a series of experiments for determining equilibrium D/H fractionation between brucite and pure water as a function of pressure at 200 to 600°C. A starting material of fine-grained brucite was reacted with excess amounts of pure water within gold capsules at elevated temperatures (200–600°C) and pressures (2.1–800 MPa). The partial-exchange method of Northrop and Clayton (1966) was employed because of likely incomplete isotopic exchange between brucite and water. A reagent-grade brucite (Alfa Products, Lot #012181, 99.2% assay with 0.5% soluble salts, ignition loss 31.3%) was used for all experiments after washing with distilled water several times and drying in a vacuum oven at 60°C for 5 d. The brucite is very fine-grained (0.1–0.5 μm), and X-ray diffraction analysis showed that brucite is the only mineral present within a detection limit of a few percent. Several isotopically different waters, ranging from $\delta D = -291.6$ to $+197.4‰$ (W-1, W-4, W-5, W-6, W-7, and W-8), were prepared by mixing an ion-exchanged local tap water, water from Antarctic ice, and small amounts of D_2O (Table 1). Between 10 and 100 mg of brucite and between 25 and 500 mg of water were sealed in 3-mm, 5-mm, or ¼-inch OD gold capsules with 0.125-mm (0.005”)

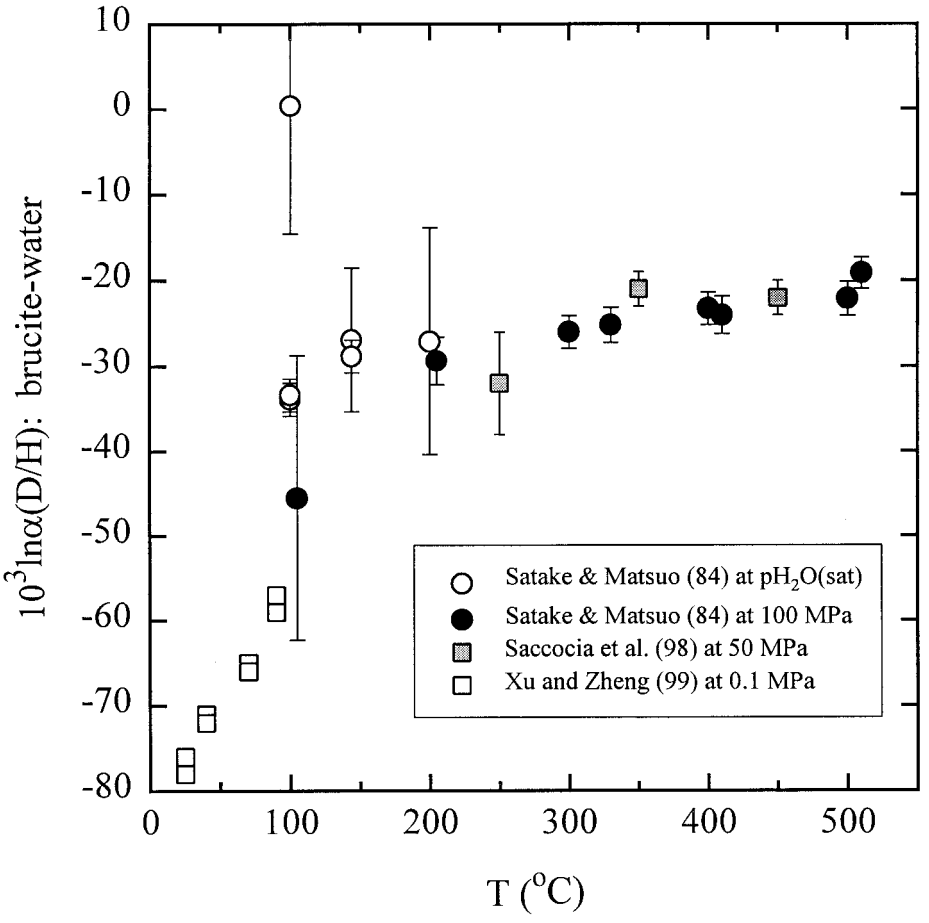

Fig. 6. Literature data of brucite-water D/H fractionation factor: Satake and Matsuo (1984) and Saccocia et al., (1998) by the partial exchange method. Saccocia et al. (1998) used 3.2 or 10 wt.% NaCl solution. Xu and Zheng (1999) synthesized by the hydrolysis of $MgCl_2$ or Mg_3N_2. Note a large discrepancy between Satake and Matsuo (1984) and Xu and Zheng (1999) at 100°C and 0.1 MPa, which cannot be ascribed to a pressure effect.

wall thickness. Water is the predominant hydrogen reservoir in the system, with hydrogen atom ratios of water to brucite ranging from 10 to 40. The Au capsules were then sealed by either cold welding or arc welding and placed in an oven overnight to check for leaks. A set of three or four such Au capsules, all the same except for the isotopic composition of water, was then placed within a pressure vessel (titanium/stainless-steel static vessel, cold-seal apparatus, or piston cyl-

Table 3. Parameters of the vibrational spectrum of brucite.

No.	General[#] fundamental frequency (cm^{-1})	Symmetry type	Frequencies (cm^{-1})	No. of oscillators	Grüneisen parameter (γ_i)	Frequency ratio upon H→D substitution
1	—	Acoustic A_{1g}(T)	170.1	1	0.220	0.9831920
2	—	Acoustic A_{1g}(T)	170.1	1	0.220	0.9831920
3	—	Acoustic A_{1g}(T)	320.2	1	0.425	0.9831920
4	280	Optic continuum E_g(T)	265.11–405.25	2	0.8100	0.9718253
5	361	Optic continuum E_u(T)	359.70–450.25	2	0.6921	0.9884439
6	416	Optic continuum E_u(R)	410.77–440.08	2	0.9609	0.7276069
7	443	Optic continuum A_{1g}(T)	440.16–510.92	1	1.4390	0.9884439
8	461	Optic continuum A_{2u}(T)	451.42–565.95	1	2.2916	0.9544390
9	725	Optic continuum E_g(R)	715.83–750.97	2	1.5447	0.7276069
10	3652	Einstein oscillator A_{1g}(internal)	3652	1	−0.0880	0.7276069
11	3688	Einstein oscillator A_{2u}(internal)	3688	1	−0.0069	0.7276069

[#], Dawson et al. (1973).

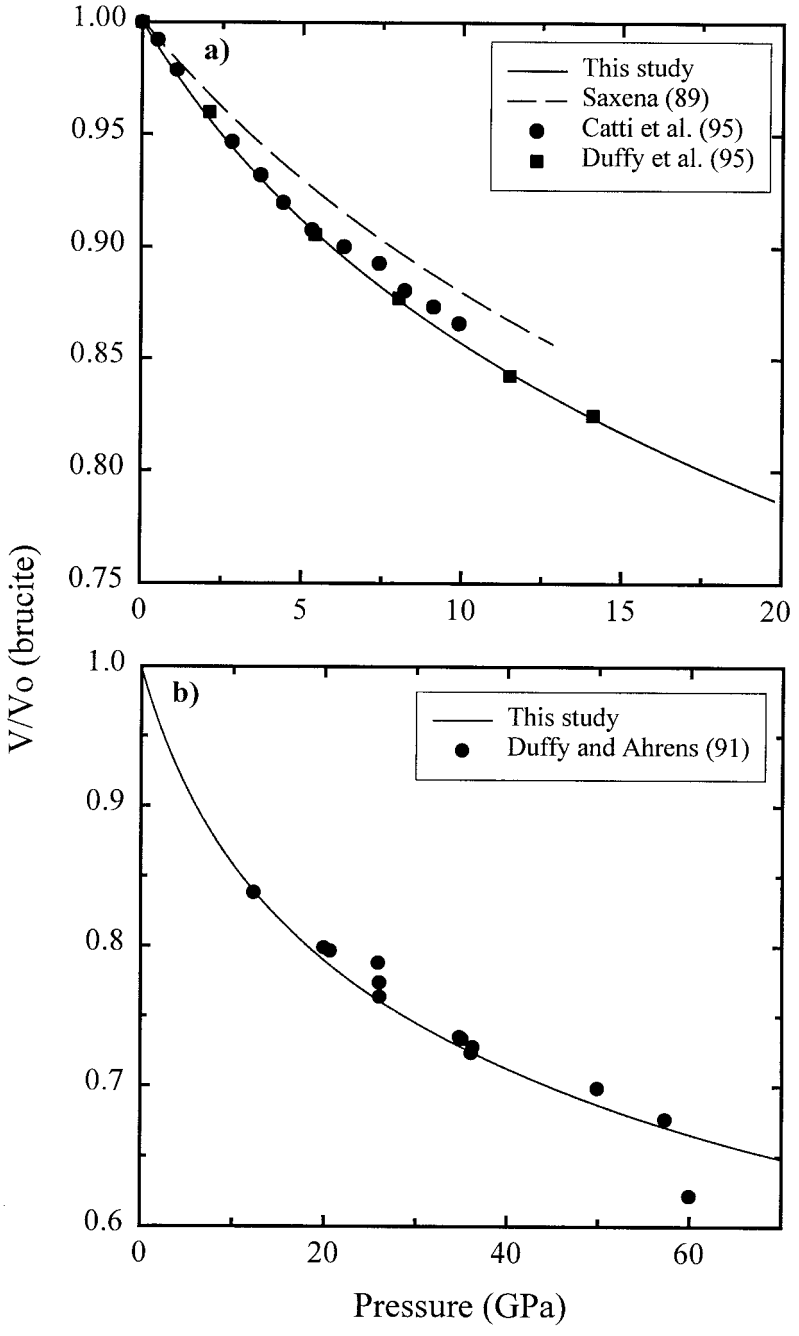

Fig. 7. Our results of (a) isothermal (300 K) and (b) shock-wave Hugoniot EOSs of brucite, compared with literature data.

inder, depending on the temperature-pressure condition of interest). Temperature and pressure of our experiments were controlled at 200 to 600°C within ± 2°C and at 2.1 to 800 MPa within ± 0.5 to 1 MPa, respectively. In two low-pressure experiments (15 and 25 MPa) at 380°C, pressure was calculated from the internal volume of the vessel and pressure-temperature-volume properties of pure water (pressure medium) to an error of ± 0.2 to 1 MPa. In the experiment with the piston cylinder at 380°C and 800 MPa, the pressure uncertainty was ± 20 MPa. We conducted a total of 20 sets of experiments over a wide range of temperature and pressure (Table 2), all in the field of liquid or supercritical water (Fig. 2). The temperature-pressure range, which we can investigate with the system brucite-water, is limited by the brucite-periclase boundary (Fig. 2). At the end of experiments for durations ranging from 283.5 to 4460 h, the vessels were quenched to below 50°C within 5 to 30 min, and the gold capsules recovered were weighed to check for leakage. Water was recovered from most of the gold capsules after the experiments. The capsules were placed in a puncture device made of Pyrex tube and threaded Teflon

Table 4. Calculated equation of state of brucite compared with the literature data.

	Heat capacity (J mole^{-1} K^{-1})		Volume (V/V$_0$)	
T (K)	Calculated	Observed[#]	Calculated	Observed[§]
300	79.38	77.94	1.0	1.0
350	86.65	85.12	1.004293	1.003962
400	92.30	90.85	1.009096	1.008553
450	96.82	95.54	1.01437	1.013773
500	100.55	99.46	1.020044	1.019622
550	103.76	102.78	1.026098	1.026099
600	106.60	105.66	1.032523	1.033205
650	109.22	108.13	1.039288	1.040940

Parameters	Calculated	Observed*
Adiabatic bulk modulus at 25°C (K_{OS}, GPa)	42.043	42.0
Pressure derivative of bulk modulus (K'_0)	5.70	5.70

[#] From Holland and Powell (1990).
[§] From Redfern and Wood (1992).
* From Duffy et al. (1995).

plunger attached with a tungsten needle. After evacuating the puncture device, the capsule was punctured by advancing the tungsten needle, and water inside was quantitatively recovered and sealed in Pyrex tubes for isotopic analysis at a later time. Then, the brucite run products were recovered from the capsules, washed with deionized water, and dried in an oven at 60°C overnight. SEM observations suggest that the brucite had undergone significant grain-coarsening (Fig. 3).

Between 6 and 10 mg of the starting material or run products of brucite were loaded in a silica cup, which was then placed inside a dehydration tube made of silica glass. After attaching the dehydration tube to a vacuum system, the brucite sample was dried at 120°C in vacuum overnight. The sample was then heated to above 900°C for 0.5 to 1 h with an electric furnace to dehydrate brucite completely. The water recovered from a brucite sample was then stored in a Pyrex tube for later isotopic analysis. A test with the starting brucite showed that δD values of water released during the dehydration did not change regardless of whether non-condensable gases were recovered or not recovered by passing over hot CuO at 600°C, suggesting that no measurable H_2 was produced. All water samples (starting waters, water run products, and water recovered from brucite samples) were converted to H_2 by passing over uranium at 750°C (Bigeleisen et al., 1952). D/H ratios of the H_2 gases were measured with a Finnigan MAT252 isotope ratio mass spectrometer, which was calibrated against a set of VSMOW and SLAP standards prepared in the same manner as the water and brucite samples. The external precision of D/H ratio measurements, based on replicate analysis of the starting brucite and waters, ranged from ± 0.1 to 0.7‰ (1σ) with an average of ± 0.34‰ (Table 1).

The δD value of water after the experiments was obtained by two methods: (a) isotope-balance calculations using the measured δD values of the initial water and brucite starting and run products, and (b) direct measurements of water run products after recovery. A comparison of the two methods shows that measured δD values of water run products are slightly lower (−1.39 ± 1.26‰, 1σ, $n = 51$) than those obtained by isotope-balance calculations (Table 2). This small discrepancy could be due to the contribution of water adsorbed onto the surface of the starting brucite and/or atmospheric moisture trapped inside Au capsules during loading. Although it is reported in the literature that hydrogen diffusion through the wall of Au capsules can alter the δD value of water inside, especially at high temperatures (Graham et al., 1987), our results showed that hydrogen diffusion was not significant even at 600°C and 300 MPa. Because δD values of water did not change much during the experiments due to large water/brucite ratios and because δD values of the water run products obtained by the two methods are in good agreement, the values obtained by isotope-balance calculations were used in this study.

Table 5. Calculations of the D/H β-factor of brucite at 0 MPa. Error is approximately ±1%..

T (K)	β-factor
300	10.9407
350	7.1936
400	5.2822
450	4.1700
500	3.4607
550	2.9770
600	2.6301
650	2.3714
700	2.1725
750	2.0156
800	1.8893
850	1.7860
900	1.7001
950	1.6280
1000	1.5666
1050	1.5140
1100	1.4685
1150	1.4288
1200	1.3940
1250	1.3634
1300	1.3362
1350	1.3120
1400	1.2903
1450	1.2708
1500	1.2532

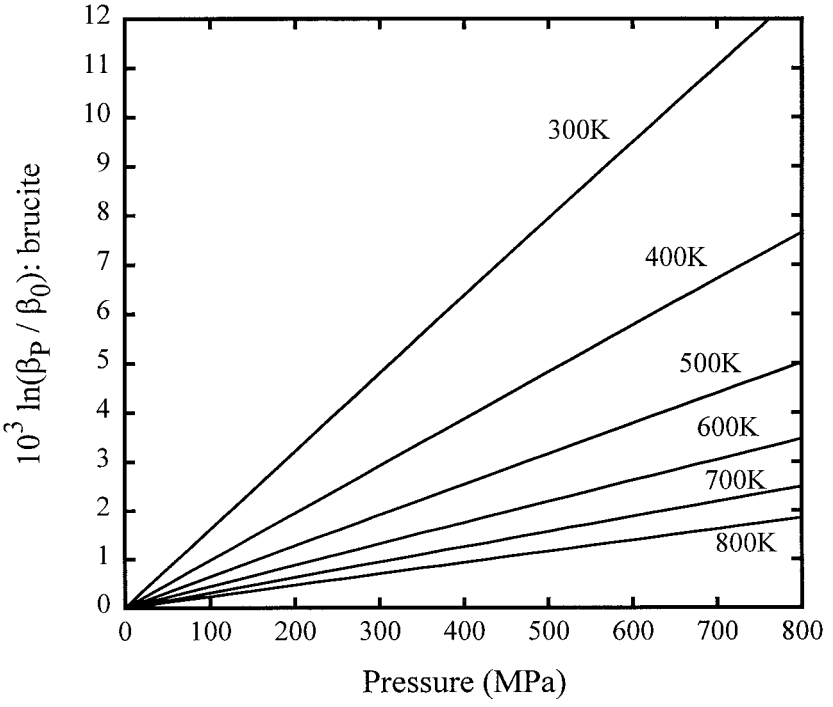

Fig. 8. Calculations of pressure effects on the D/H β-factor of brucite (Table 6).

4.2. Results

The isotopic analysis of the run products showed that brucite and water did not reach isotopic equilibrium at the experimental conditions. Thus, the equilibrium D/H fractionation factor between brucite and water was calculated by means of the partial exchange method developed by Northrop and Clayton (1966) and Suzuoki and Epstein (1976). We prepared three to four Au capsules with water of different D/H ratios as discussed above, so that the validity of the partial exchange technique and associated statistical errors could be rigorously evaluated. The value of $10^3(\alpha_{eq}-1)$ was calculated from a linear regression of a set of three or four data, taking into account both goodness of fit and analytical errors of the isotopic data (York, 1969; Ludwig, 1994). These values were then converted to the value of $10^3\ln\alpha_{eq}$. Calculated fractions of isotopic exchange between brucite and water (89–99%) are consistent with observed significant grain-coarsening of the starting brucite, and net isotope exchange was most likely promoted by dissolution-precipitation process (Ostwald ripening). Good linear fitting of each set of experimental data and the high degree of isotopic exchange resulted in good precision of calculated values of the D/H fractionation factor ($\pm$ 0.72 to $\pm$ 2.48‰ with $\pm$ 1.15‰, on average, 1σ, and $n = 20$) (Table 2 and Fig. 4).

Experimental results on equilibrium D/H fractionation between brucite and water obtained in this study are shown in Figure 5. At all the temperatures (200, 300, 380, 500, and 600°C), the measured values of $10^3\ln\alpha$ for D/H fractionation between brucite and water increased with increasing pressure, especially at $\leq$ 100 MPa. The magnitude of the observed pressure effects ranges from 4.4‰ at 600°C and 100 to 300 MPa to 12.4‰ at 380°C and 11 to 800 MPa. The observed pressure effects on the value of $10^3\ln\alpha_{eq}$ are more pronounced in the low-pressure range ($<$ 100 MPa) than in the high-pressure range ($>$ 100 MPa) (Fig. 5a). When the same results are plotted as a function of the density of pure water at experimental conditions (Haar et al., 1984), a good linear relation was observed at each temperature (Fig. 5b). Satake and Matsuo (1984) were the first to determine equilibrium D/H fractionation factors between brucite and water at 100 to 510°C, using the partial exchange method. Their results at 200, 300, and 500°C, all at 100 MPa, are consistent with our results within error, although their values appear slightly (1–2‰) greater than our values (Fig. 5b). Note that we recalculated the equilibrium $10^3\ln\alpha$ values and associated errors from data presented by Satake and Matsuo (1984), because they did not propagate analytical errors properly and because their tabulated results contained errors (Satake, pers. comm.). Saccocia et al., (1998) also determined $10^3\ln\alpha$ values between brucite and 3.2 or 10 wt.% NaCl solutions at 250, 350, and 450°C, all at 50 MPa. Their results agree with those of Satake and Matsuo (1984) (Fig. 6). Xu and Zheng (1999) investigated D/H isotopic fractionation during the hydrolysis of $MgCl_2$ and Mg_3N_2 to $Mg(OH)_2$ in the temperature range from 25 to 90°C at 0.1 MPa. Xu and Zheng (1999) argued that consistent results obtained by the two reaction pathways suggest the attainment of isotopic equilibrium, and that a discrepancy (13‰) between their results at 90°C and 0.1 MPa and those of Satake and Matsuo (1984) at 105°C and 100 MPa is due to the pressure effect (Fig. 6). However, our error analyses of the results by Satake and Matsuo (1984) showed that their data at 105°C and 100 MPa has a large error ($\pm$ 17‰, 1σ) due to a low percentage ($<$ 10%) of isotopic exchange (Fig. 6). In fact, their precise results at

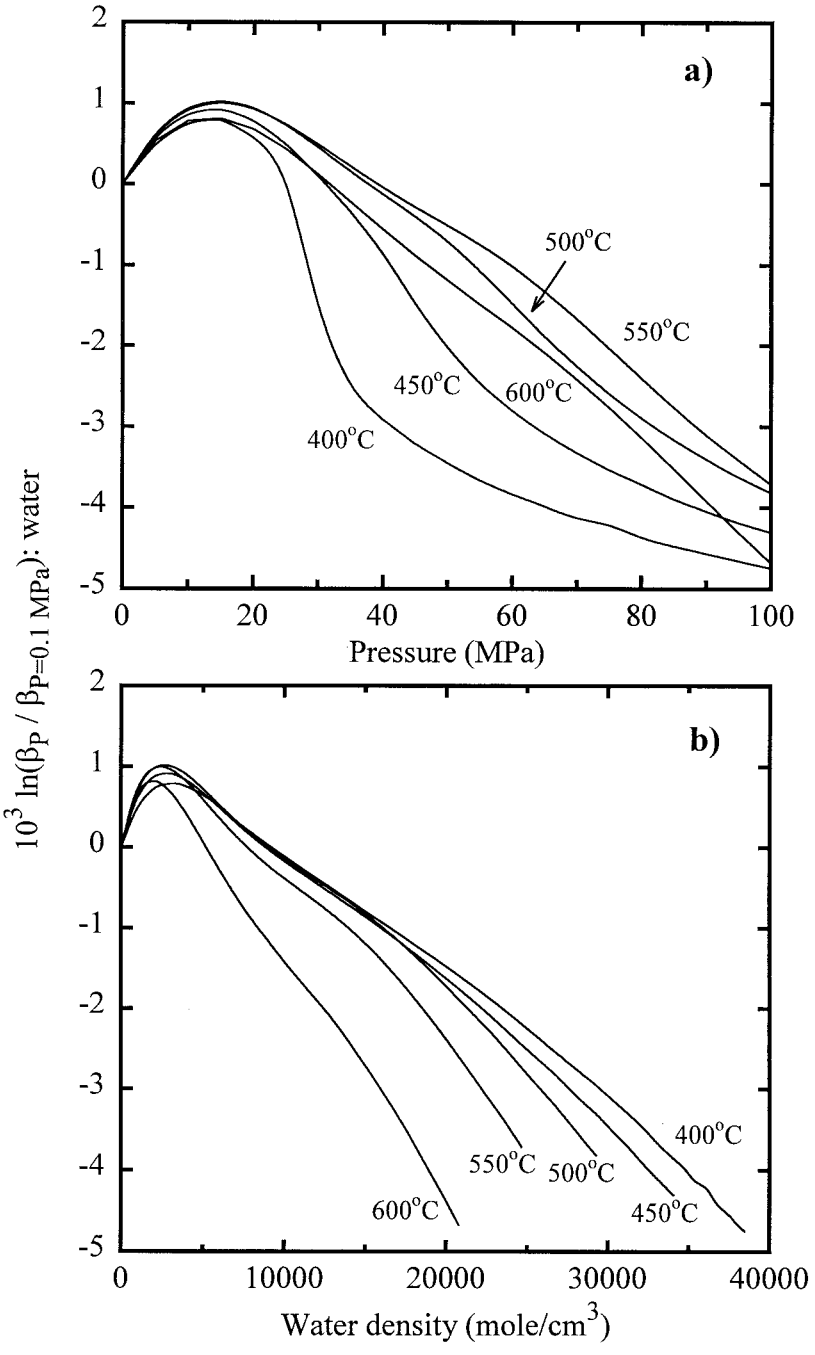

Fig. 9. Calculations of pressure effects on the D/H β-factor of water as a function of (a) pressure and (b) density of water (Polyakov et al., in prep.).

100°C (-33.6 ± 1.9‰) were obtained at 0.1 MPa, which in turn were ~25‰ greater than those of Xu and Zheng (1999) at 90°C and 0.1 MPa. Therefore, the large discrepancy between the two studies at 90 to 100°C and 0.1 MPa cannot be the result of the pressure effect. During the hydrolysis reactions of $MgCl_2$ and Mg_3N_2 employed by Xu and Zheng (1999), a disproportionation reaction must have occurred: $Mg^{2+}(aq) + 2H_2O \rightarrow Mg(OH)_2 + 2H^+$. It is very likely that kinetic isotopic fractionations accompanied these disproportionation reactions.

A very good linear relation was observed between $10^3 \ln\alpha$ and the density of water even for a wide range of densities at 380°C (0.070–1.035 g/cm^3) (Fig. 5b). The density of water is very well constrained (< 0.005 g/cm^3) except near the critical point of water (374°C and 22 MPa) at 380°C and 20 MPa, where the uncertainty due to errors in temperature and pressure produced an error in density as large as $\pm$ 0.05 g/cm^3. We calculated coefficients of a linear regression at each temperature, taking into account errors in both calculated $10^3 \ln\alpha$ values and the density of water (York, 1969; Ludwig, 1994) (all errors are in 1σ):

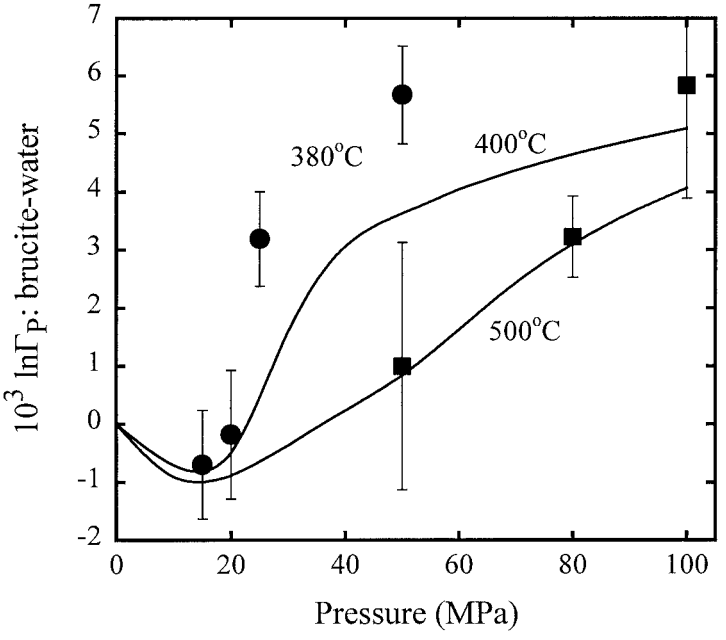

Fig. 10. Comparison of experimental and theoretical results of pressure effects on brucite-water D/H fractionation factor (for the definition of $10^3\ln\Gamma_P$, see Eqn. 3 to Eqn. 6): solid lines, calculations at 400 and 500°C; solid circles and squares, experiments at 380 and 500°C, respectively. The experimental values were shifted by +31.2 and +28.0‰ for 380 and 500°C data, respectively, for comparison of the magnitude of the effects.

$$10^3\ln\alpha_{\text{Brucite-Water}} = 46.4(\pm 8.5)\rho_{\text{Water}} - 75.4(\pm 7.9) \text{ at } 200°\text{C} \quad (13)$$

$(0.865 \leq \rho_{\text{Water}} \leq 1.01,\ n = 2)$

$$10^3\ln\alpha_{\text{Brucite-Water}} = 24.0(\pm 7.4)\rho_{\text{Water}} - 48.2(\pm 6.1) \text{ at } 300°\text{C} \quad (14)$$

$(0.717 \leq \rho_{\text{Water}} \leq 0.929,\ n = 4)$

$$10^3\ln\alpha_{\text{Brucite-Water}} = 10.6(\pm 1.4)\ \rho_{\text{Water}} - 32.7(\pm 0.8) \text{ at } 380°\text{C} \quad (15)$$

$(0.070 \leq \rho_{\text{Water}} \leq 1.035,\ n = 6)$

$$10^3\ln\alpha_{\text{Brucite-Water}} = 15.0(\pm 3.9)\rho_{\text{Water}} - 31.7(\pm 2.2) \text{ at } 500°\text{C} \quad (16)$$

$(0.47 \leq \rho_{\text{Water}} \leq 0.773,\ n = 4)$

$$10^3\ln\alpha_{\text{Brucite-Water}} = 15.2(\pm 4.6)\rho_{\text{Water}} - 30.9(\pm 2.7) \text{ at } 600°\text{C} \quad (17)$$

$(0.410 \leq \rho_{\text{Water}} \leq 0.696,\ n = 3)$

where ρ_{Water} is the density of water (g/cm^3). It appears that the slope decreases with temperature from 200 to 380°C, whereas the intercept increases with temperature from 200 to 600°C. The slopes at temperatures of 380, 500, and 600°C are indistinguishable within errors. These good linear relations can be used to calculate D/H fractionation factors between brucite and water within pressure ranges of this study. However, an extrapolation of these equations beyond the pressure ranges of this study may not be advisable.

5. THEORETICAL STUDY

5.1. Brucite

Polyakov and Kharlashina (1994) were the first to calculate pressure effects on the D/H reduced partition function ratios (β-factor) of brucite, based on the model developed by Kieffer (1979, 1980, 1982). Here, we further improved a Kieffer-type model for calculating pressure effects on the D/H β-factor of brucite by incorporating recent experimental results on the pressure dependency of IR and Raman spectra of brucite at high pressures. Similar models have been successfully applied to the calculation of thermodynamic properties of solids, using IR and Raman spectroscopic data (Gillet et al. 1996), the β-factors of minerals (Kieffer, 1982), and their pressure dependencies, "the isotope pressure effects" (Polyakov and Kharlashina, 1994; Polyakov 1998).

The vibration spectrum of brucite consists of 15 branches (Table 3). Dawson et al. (1973) identified and assigned all IR and Raman active modes of brucite. Thus, all fundamental frequencies of brucite, except for acoustic modes, are known. Following Kieffer (1979), we described the distribution of three acoustic modes by assuming the sine-wave dispersion. Two internal optic modes assigned to OH-group-stretching vibrations were simulated by two Einstein oscillators. Six remaining optic vibrational branches (four are doubly degenerated) were presented by uniform distribution over the range, including the value of fundamental frequency. The isotope frequency ratios of fundamental normal modes were calculated based on the group theory from their symmetry types and displacements obtained from Mitra (1962). The isotopic frequency ratios and Grüneisen parameters were assigned for every component of the vibration spectrum (Table 3).

Table 6. Calculations of pressure effects on the D/H β-factor of brucite. Error is approximately ±5–10%.

	$10^3\ln(\beta_P/\beta_0)$										
	T (K)										
Pressure (MPa)	300	350	400	450	500	550	600	650	700	750	800
0	0	0	0	0	0	0	0	0	0	0	0
25	0.41	0.31	0.25	0.20	0.16	0.14	0.11	0.09	0.08	0.06	0.06
50	0.81	0.62	0.49	0.39	0.32	0.27	0.22	0.19	0.15	0.13	0.12
75	1.21	0.93	0.74	0.59	0.48	0.40	0.33	0.28	0.23	0.20	0.18
100	1.61	1.24	0.98	0.78	0.64	0.53	0.44	0.37	0.31	0.27	0.23
125	2.01	1.55	1.22	0.98	0.80	0.66	0.55	0.47	0.39	0.34	0.29
150	2.41	1.86	1.47	1.17	0.96	0.79	0.66	0.56	0.47	0.40	0.35
175	2.81	2.17	1.71	1.37	1.12	0.93	0.77	0.65	0.55	0.47	0.41
200	3.21	2.47	1.95	1.56	1.28	1.06	0.88	0.74	0.63	0.54	0.47
225	3.61	2.78	2.19	1.76	1.44	1.19	0.99	0.84	0.71	0.61	0.53
250	4.01	3.09	2.43	1.95	1.59	1.32	1.10	0.93	0.79	0.67	0.58
275	4.40	3.39	2.67	2.14	1.75	1.45	1.21	1.02	0.87	0.74	0.64
300	4.80	3.70	2.92	2.34	1.91	1.58	1.32	1.11	0.94	0.81	0.70
325	5.19	4.00	3.16	2.53	2.07	1.71	1.43	1.21	1.02	0.88	0.76
350	5.59	4.31	3.40	2.72	2.22	1.84	1.54	1.30	1.10	0.94	0.82
375	5.98	4.61	3.63	2.92	2.38	1.97	1.64	1.39	1.18	1.01	0.87
400	6.38	4.91	3.87	3.11	2.54	2.10	1.75	1.48	1.26	1.08	0.93
425	6.77	5.22	4.11	3.30	2.69	2.23	1.86	1.57	1.33	1.14	0.99
450	7.16	5.52	4.35	3.49	2.85	2.36	1.97	1.66	1.41	1.21	1.05
475	7.55	5.82	4.59	3.68	3.01	2.49	2.08	1.76	1.49	1.28	1.11
500	7.94	6.12	4.83	3.87	3.16	2.62	2.19	1.85	1.57	1.34	1.16
525	8.33	6.42	5.06	4.06	3.32	2.75	2.29	1.94	1.65	1.41	1.22
550	8.72	6.72	5.30	4.25	3.47	2.87	2.40	2.03	1.72	1.48	1.28
575	9.11	7.02	5.54	4.44	3.63	3.00	2.51	2.12	1.80	1.54	1.34
600	9.50	7.32	5.77	4.63	3.78	3.13	2.62	2.21	1.88	1.61	1.39
625	9.88	7.62	6.01	4.82	3.94	3.26	2.72	2.30	1.96	1.68	1.45
650	10.27	7.92	6.25	5.01	4.09	3.39	2.83	2.39	2.03	1.74	1.51
675	10.66	8.22	6.48	5.20	4.25	3.51	2.94	2.48	2.11	1.81	1.57
700	11.04	8.52	6.72	5.39	4.40	3.64	3.04	2.57	2.19	1.88	1.62
725	11.43	8.81	6.95	5.58	4.56	3.77	3.15	2.66	2.26	1.94	1.68
750	11.81	9.11	7.18	5.77	4.71	3.90	3.26	2.75	2.34	2.01	1.74
775	12.20	9.41	7.42	5.96	4.86	4.02	3.36	2.84	2.42	2.07	1.79
800	12.58	9.7	7.65	6.14	5.02	4.15	3.47	2.93	2.49	2.14	1.85

To calculate the equation of state (EOS) and thermodynamic properties of solids, the knowledge of the static part of free energy is needed. The Helmholtz free energy (F) can be written as the sum of two parts (e.g., Born and Huang, 1954):

$$F\ (V,\ T) = F_{\text{pot}}(V) + F_{\text{vib}}\ (V,T), \qquad (18)$$

where F_{pot} is the potential Helmholtz free energy, which is an explicit function of volume. F_{pot} describes the volume dependence of the potential energy of a static crystalline lattice. F_{vib} is the thermal (vibrational) Helmholtz free energy, which generally depends on temperature and volume. We approximate the volume dependence of the free energy using the Born-Mayer potential function model:

$$F_{Pot} = \frac{3V_0A}{B}\exp[B(1 - X^{1/3})] - 3V_0KX^{1/3}, \qquad (19)$$

where A, B, and K are parameters of the potential function, V_0 the molar volume at standard condition (T = 298.15 K, P = 0.1 MPa) and $X = V/V_0$. Parameters for the Born-Mayer potential, as well as those for the vibrational spectrum, were obtained by fitting the following experimental input data: heat capacity at constant pressure, C_P(T); density (volume) at normal pressure, ρ(T); bulk modulus at 25°C and normal pressure, K_0; and the pressure derivative of the bulk modulus at 25°C and normal pressure, K' (Holland and Powell, 1990; Redfern and Wood, 1992; and Duffy et al., 1995). During fitting, the frequencies and Grüneisen parameters of the internal vibration modes were fixed equal to their experimental values obtained from Duffy et al., (1995) and Kruger et al. (1989) as well as Grüneisen parameters of E_g(T) and A_{1g}(T) modes. Details of the fitting procedure were previously presented by Polyakov and Kuskov (1995). Parameters of the Born-Mayer potential function obtained by the fitting are A = 11.6819 GPa, B = 12.2 GPa, and K = 13.8002 GPa. Calculated parameters of the vibrational spectrum are presented in Table 3, and the input and calculated parameters for the EOS are compared in Table 4. The EOS obtained from our model agrees well with the isothermal and the shock-wave EOSs in the literature (Fig. 7). In addition, our calculation yielded a standard entropy of 62.95 J/(mol K), which is in excellent agreement with that experimentally obtained of 63.00 J/(mol K) (Holland and Powell, 1990). Thus, our brucite model can calculate satisfactorily both the thermodynamic properties and the EOS.

This new brucite model was used to calculate the β-factor of brucite. Changes in the vibrational frequency of brucite with D/H isotopic substitution were calculated using the normal

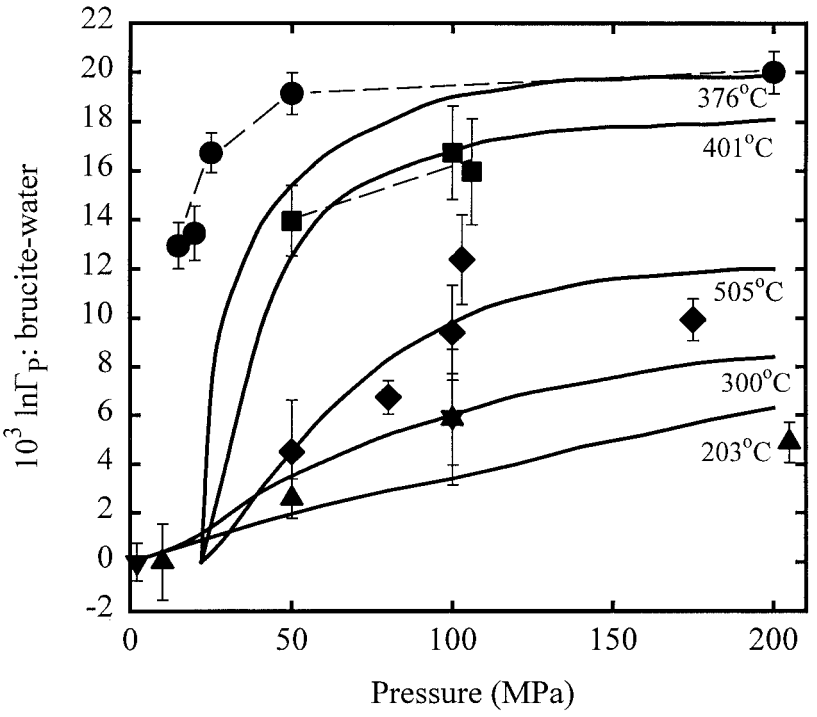

Fig. 11. Comparison of experimental results of pressure effects on brucite-water D/H fractionation factors and on the β-factor of water calculated by Driesner (1997) (for the definition of $10^3 \ln\Gamma_P$, see Eqn. 3-6): solid lines-calculations and solid symbols-experiments (inverse triangle, 200°C; triangle, 300°C; circle, 380°C; square, 400°C; diamond, 500°C). The experimental values were shifted for comparison.

mode displacements given by Mitra (1962). Following Kieffer (1982), we assumed that the isotopic frequency ratio of the acoustic modes is equal to the square-root of the ratio of isotopic molecular masses:

$$\frac{\nu^*}{\nu} = \sqrt{\frac{m_{Mg} + 2m_o + 2m_H}{m_{Mg} + 2m_o + 2m_D}}, \tag{20}$$

where ν and ν^* are the acoustic frequencies of $Mg(OH)_2$ and $Mg(OD)_2$, respectively. The m_{Mg}, m_o, m_H, and m_D are atomic masses of magnesium, oxygen, protium, and deuterium, respectively. Results of our calculations of D/H β-factors for brucite have an error of approximately $\pm$ 1% (Table 5).

Pressure effects on the D/H β-factors of brucite were calculated using the quasi-harmonic approximation. Within this approximation, vibrational frequencies are a function of volume. This volume dependence is defined by the modal Grüneisen parameter,

$$\gamma_i = -\left(\frac{\partial \ln \nu_i}{\partial \ln V}\right)_T \tag{21}$$

At a given temperature and pressure, an appropriate value of the molar volume (V) was calculated using the model presented above. Then, we calculated the value of the D/H β-factor, using the vibrational frequencies calculated from Eqn. 21. It should be noted that frequency shifts caused by isotopic substitution were assumed independent of pressure (or volume). Details of these calculations were previously presented by Polyakov (1998).

The results of our calculations for the isotope pressure effects have an error of $\pm$ 5 to 10% (Table 6 and Fig. 8). The D/H β-factor of brucite increases linearly with pressure at least up to 800 MPa. This can be explained by linear dependency of the density of brucite on pressure. The pressure effects on the D/H β-factor of brucite decrease with increasing temperature. The relatively small pressure effects at elevated temperatures can be explained by negative values of the modal Grüneisen parameter for two high-frequency stretch modes.

5.2. Water

Using the relation between the β-factor and MVIE (Eqn. 9), Polyakov and Kharlashina (1994) calculated the D/H pressure effects on water along the liquid-vapor water boundary. They used molar volume data of water presented by Rabinovich (1970). We extended this same approach to a wider temperature-pressure range using updated equations of state for H_2O and D_2O. Because we assumed the ideal mixing of H_2O and D_2O, our calculations are not valid near the critical point of water (374°C and 22.1 MPa), where the molar volumes of H_2O and D_2O differ by more than 12%. For the calculation of the molar volume of HDO, the rule of geometric mean was employed, i.e., $n = 2$ in Eqn. 9. The deviation from the geometric mean rule is small for water ($<$6%) (Rabinovich, 1970; Jancsó and Jákli, 1980; Jákli and Van Hook, 1981; Jancsó et al., 1993). This simple approach does not require models for the intermolecular interactions of water, and details of our calculations are presented by Polyakov et al., (in prep.).

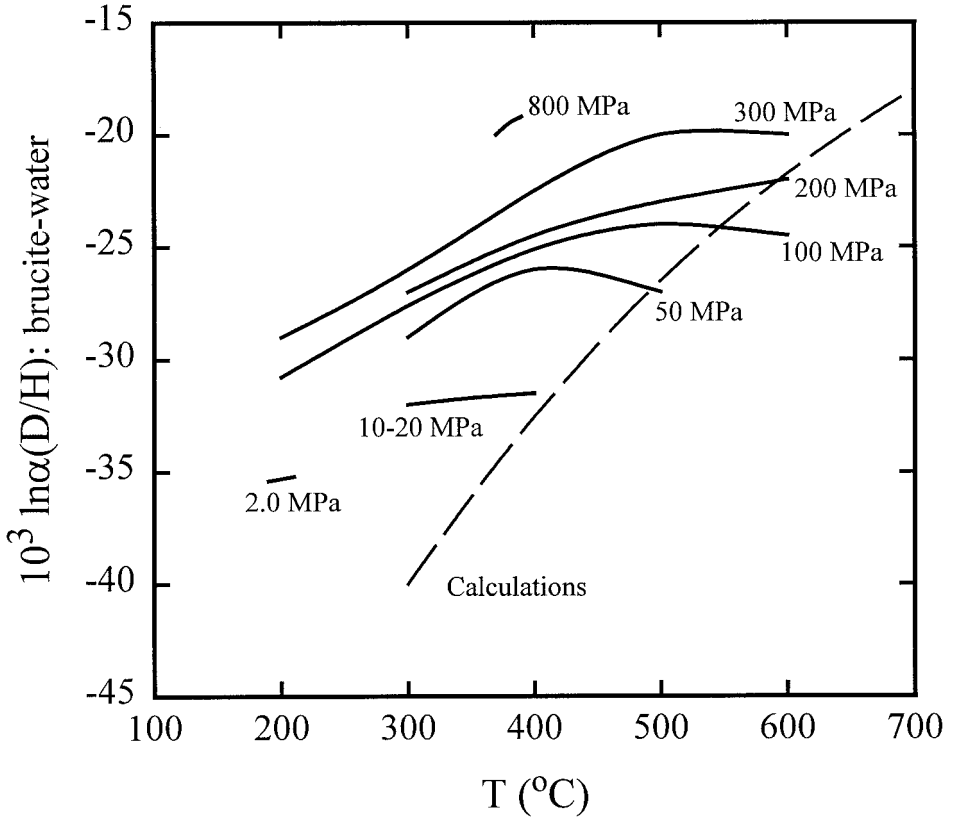

Fig. 12. Brucite-water D/H fractionation as a function of temperature and pressure. The calculated values, based on statistical-mechanically calculated β-factors of brucite at 0.0 MPa in this study (Table 5) and of water by Richet et al. (1977), have large errors ($\pm$ 20‰ at 300°C to $\pm$ 15‰ at 700°C). The isobaric fractionation curves are constructed based on experimental results in this study and by Satake and Matsuo (1984).

We first calculated the P-V-T properties of ordinary and heavy water in the range of 400 to 600°C and 0 to 100 MPa. The EOSs were obtained from Kestin et al., (1984a, b) for H_2O, and Hill et al. (1982) and Hill (1990) for D_2O. The temperature-pressure range for this calculation was limited by the range of EOS for D_2O and by the critical points of water. The EOSs, which are presented in the form of canonical equations by these investigators, were solved numerically. Uncertainty in the specific volume is ~0.01% for D_2O (Hill et al., 1982), which is an order of magnitude larger than that of H_2O. Then, the pressure-derivative of the β-factor was calculated using Eqn. 9. The uncertainty in the specific volumes of D_2O and H_2O leads to a $\pm$ 5% error in the calculated values of $10^3\Delta\ln\beta = 10^3\ln(\beta_P/\beta_{P=0.1\ MPa})$. Our calculations show that at 400 to 600°C, the β-factor of water slightly (1‰) increases with increasing pressure to 15 MPa, and then decreases by as much as 4 to 5‰ with increasing pressure to 100 MPa (Fig. 9a). The cause of slight increases in the low-pressure range is not clear. Pressure effects on the D/H β-factor of water appear to flatten out with pressure in a similar fashion to the pressure effects on $10^3\ln\alpha$ values for brucite-water (Fig. 5a). The D/H β-factor of water appears to decrease linearly with the density of water (Fig. 9b) as $10^3\ln\alpha$ values for brucite-water D/H fractionation increased linearly with the density of water (Fig. 5b). The statistical-mechanical calculations of Driesner (1997), based on red shifts of symmetric O-H stretching frequency of water with pressure (Frantz et al., 1993), also showed large decreases in the D/H β-factor of water at temperatures from 200 to 500°C and pressures to 200 MPa. However, the magnitude of his pressure effects on the β-factor of water (up to 20‰) is two to four times that of our calculations at a given temperature.

6. DISCUSSION

Our experimental results of the pressure effects on brucite-water D/H fractionation can now be compared with our calculations of the pressure effects on brucite and water. Figure 10 shows these calculated overall pressure effects on brucite-water D/H isotope fractionation, which were obtained by combining the pressure effects on the β-factor of brucite and water calculated separately (Figs. 8, 9). The overall D/H isotope pressure effect in the system brucite-water increases by ~5‰ with increasing pressure to 100 MPa at 400 to 600°C, due to a combination of the positive and negative pressure effects on the D/H β-factor of brucite and water, respectively. Our experimental results on brucite-water D/H fractionation in the same temperature (380–400 and 500°C) and pressure range are also shown for comparison. Because our experiments were not conducted at a reference pressure, 0.0 and 0.1 MPa for brucite and water, respectively, the measured $10^3\ln\alpha$ values are arbitrarily (+31.2 and +28.0‰ for 380 and 500°C, respectively)

shifted, so that the magnitude of experimental and theoretical results of pressure effects on brucite-water D/H fractionation can be readily compared. Considering analytical errors and potential uncertainties in the calculations, the agreement in the magnitude of the D/H isotope pressure effects between the experimental results and calculations is excellent (Fig. 10). The results of our theoretical calculations of the isotope pressure effects on the system brucite-water not only corroborate our experimental results, but also demonstrate that the observed D/H isotope pressure effects on the system brucite-water under temperature-pressure conditions of this study originate largely from the isotope pressure effects on water.

We also compared our experimental results with Driesner (1997), who calculated the D/H isotope pressure effects on water only based on Raman spectra of water at elevated temperatures and pressures. Driesner (1997) did not calculate pressure effects on the D/H-reduced partition function ratio for brucite. Driesner's calculations also agree reasonably well with our experimental results (Fig. 11). The pressure effects are large at pressures below 100 MPa and flatten out at higher pressures. The magnitude of the calculated pressure effects is a factor of two to three larger than those of our experimental results at 376 to 380°C, but the agreement is good at 200, 300, 400, and 500°C (Fig. 11).

The limited temperature-pressure range (up to 600°C and 100 MPa) of the available molar volume data of D_2O (Hill et al., 1982; Hill, 1990) precluded our calculations of the isotope pressure effects on water at higher pressures and temperatures. However, the good linear relation observed between the calculated pressure effects on the D/H β-factor and the density of water above 3000 mol/cm^3 (Fig. 9) may be used to evaluate the isotope pressure effects on water outside of this P-T range. The density of water, which is well determined to high temperatures (up to 1100°C) and high pressures ($>$ 3.0 GPa) (Larrieu and Ayers, 1997; Withers et al., 2000), is probably the best proxy for the D/H pressure effect of water. The density of water (and probably also the D/H pressure effect of water) flattens out with pressure. On the other hand, the pressure effect on brucite increases linearly with pressure (Fig. 8). These observations suggest that the magnitude of the isotope pressure effect on brucite eventually exceeds that of water at high pressures, perhaps above 2 GPa, and that the overall D/H fractionation between brucite and water at very high pressures increases linearly with pressure.

The value of $10^3\ln\alpha$ between brucite and water can also be obtained from statistical-mechanical calculations of the β-factors of brucite (Table 5) and water (Richet et al., 1977). Because the brucite data in Table 5 was calculated at 0.0 MPa and the those for water was calculated ignoring intermolecular interactions of water molecules, calculated $10^3\ln\alpha$ values for brucite-water would represent those at very low pressures. The calculated $10^3\ln\alpha$ values have large errors ($\pm$ 100‰ at room temperature to $\pm$ 10‰ at 1000°C), because the β-factors of brucite in Table 5 are large, especially at low temperatures, with an error of $\pm$ 1%. Considering these large errors, agreement is reasonable between the $10^3\ln\alpha$ values calculated from statistical-mechanics and those experimentally determined in this study (Fig. 12).

Because MVIE between H_2O and D_2O is inverse, $V(D_2O) > V(H_2O)$, the D/H β-factor of water decreases with pressure as discussed above. This is a main cause of the observed pronounced pressure effects on the overall D/H fractionation factor (Fig. 5). On the other hand, limited molar volume data of $H_2{}^{18}O$ at temperatures to 80°C and at 0.1 MPa (Kell, 1977) suggest that MVIE of $H_2{}^{16}O$ and $H_2{}^{18}O$ is normal, $V(H_2{}^{16}O) > V(H_2{}^{18}O)$. If the $^{18}O/^{16}O$ isotope pressure effect on water is similar in magnitude to those of other compounds, pressure will have a minor effect on the overall $^{18}O/^{16}O$ isotope fractionation factors between water and other compounds. This might explain why no measurable $^{18}O/^{16}O$ isotope pressure effects were observed in several mineral (quartz, calcite, albite, wollastonite)-water systems at temperatures as low as 400°C and at pressures as high as 2.2 GPa, as discussed under "Previous Studies" (above), despite the fact that Polyakov and Kharlashina (1994) and Polyakov (1998) calculated as much as a +0.5‰ $^{18}O/^{16}O$ isotope pressure effect on minerals alone under these conditions.

7. GEOCHEMICAL IMPLICATIONS

We have clearly demonstrated that pressure affects D/H isotope fractionation in the system brucite-water. Fig. 12 shows our current knowledge of the temperature and pressure dependence of the brucite-water D/H fractionation factor. At a constant pressure, the D/H fractionation is only slightly temperature-dependent (smaller than 10‰ variation) at 200 to 600°C. In contrast, the D/H fractionation factor increases ~15‰ with increasing pressure to 800 MPa at 380°C. Thus, the observed pressure effects on brucite-water D/H fractionation are greater than the observed temperature effects (Fig. 12). Results of our theoretical calculations showed that pressure effects on brucite-water D/H fractionation result largely from those on water rather than effects on brucite. Thus, it is very likely that D/H fractionation of any hydrous mineral-water systems is subject to similar, if not the same, pressure effects of those observed in the system brucite-water.

As discussed above, it is well recognized that there exist large (10–60‰) discrepancies in many hydrous mineral-water D/H fractionations studied by different investigators at different pressures (Fig. 1). Now we can assess whether these discrepancies could be explained in terms of the isotope pressure effect. Studies conducted at higher pressures invariably yielded greater D/H fractionation factors of a given hydrous mineral-water system than those conducted at lower pressures. This relation is consistent with the D/H isotope pressure effect demonstrated in a brucite-water system in this study. However, the discrepancies among different studies in the literature are much larger than those estimated from Eqn. 13 through Eqn. 17. Only about one-tenth to one-half of the differences among different experimental studies conducted for various hydrous minerals (serpentine, epidote, tourmaline, hornblende, and boehmite) in Fig. 1 can be explained by the pressure effect.

Several mineral-water D/H fractionation factors in the literature are rather insensitive to temperature (Figs. 1, 6). However, pressure changes alone can shift significantly mineral-water D/H fractionation factors as shown for the system brucite-water (Fig. 12). The isobaric fractionation curves of the $10^3\ln\alpha$ values were constructed based on our experimental results and those by Satake and Matsuo (1984): The latter

values were slightly (−2‰) adjusted because of a systematic difference between the two data sets (Fig. 5b). Thus, if not taken into account, pressure variations could lead to large errors in the estimation of the isotopic composition of the fluid (≥ 10‰ in δD) or estimated formation temperature (≥ 100°C in calculated temperatures). Our previous experimental efforts have also demonstrated that dissolved salts in aqueous fluids can change significantly the isotopic fractionation between water and other phases (steam or minerals) even at elevated temperatures ("the isotope salt effect") (Horita et al., 1993a, b, 1995). It has become clear that in addition to temperature, pressure and fluid composition are important variables in determining equilibrium isotope fractionation factors between aqueous fluids and other phases in a wide range of temperature:

$$\alpha_{A\text{-}Water} = f(\mathrm{T}, \mathrm{P}, \mathrm{X}_{\mathrm{fluid}}) \quad (22)$$

In low-pressure (≤ 100 MPa), high-salinity (≥ 10 wt.%) environments (sedimentary basin, deep geothermal system, and ore fluids), pressure and fluid composition may be at least as important as temperature in determining isotopic fractionations. It may also be possible to use hydrous minerals-water systems as single-mineral isotope geothermometer-geobarometer, if it is proven that $^{18}O/^{16}O$ isotope fractionation is practically pressure-independent.

Acknowledgments—We acknowledge comments by B. E. Taylor and T. W. Vennemann. This research was sponsored by the Division of Chemical Sciences, Geosciences, and Biosciences, Office of Basic Energy Sciences, U.S. Department of Energy under contract DE-AC05-00OR22725, Oak Ridge National Laboratory, managed and operated by UT-Battelle, LLC (JH and DRC), and by a postdoctoral fellowship from the Swiss National Science Foundation (TD).

Associate editor: B. E. Taylor

REFERENCES

Bai T. B. and Koster van Groos A. F. (1998) Phase relations in the system MgO-NaCl-H_2O: The dehydroxylation of brucite in the presence of NaCl-H_2O fluid. *Am. Mineral.* **83,** 205–212.

Bigeleisen J. and Mayer M. G. (1947) Calculation of equilibrium constants for isotope exchange reactions. *J. Chem. Phys.* **15,** 261–267.

Bigeleisen J., Perlman M. L., and Prosser H. C. (1952) Conversion of hydrogenic materials to hydrogen for isotopic analysis. *Anal. Chem.* **24,** 1356–1357.

Blamart D., Pichavant M., and Sheppard S. M. F. (1989) Experimental determination of the D/H isotopic fractionation between tourmaline and water at 600, 500°C and 3 kbar. *C. R. Acad. Sci. Paris* **308 Ser II,** 39–44.

Born M. and Huang K. (1954) *Dynamical Theory of Crystal Lattices*. Clarendon Press, Oxford.

Chacko T., Riciputi L. R., Cole D. R., and Horita J. (1999) A new technique for determining equilibrium hydrogen isotope fractionation factors using the ion microprobe: Application to the epidote-water system. *Geochim. Cosmochim. Acta* **63,** 1–10.

Clayton R. N., Goldsmith J. R., Karel K. J., Mayeda T. K., and Newton R. C. (1975) Limits on the effect of pressure on isotopic fractionation. *Geochim. Cosmochim. Acta* **39,** 1197–1201.

Clayton R. N., Goldsmith J. R., and Mayeda T. K. (1989) Oxygen isotope fractionation in quartz, albite, anorthite and calcite. *Geochim. Cosmochim. Acta* **53,** 725–733.

Catti M., Ferraris G., Hull S., and Pavese A. (1995) Static compression and H disorder in brucite, $Mg(OH)_2$, to 11 GPa: A powder neutron diffraction study. *Phys. Chem. Miner.* **22,** 200–206.

Dawson P., Hadfield C. D., and Wilkinson G. R. (1973) The polarized infra-red and Raman spectra of $Mg(OH)_2$ and $Ca(OH)_2$. *J. Phys. Chem. Solids* **34,** 1217–1225.

Driesner T. (1997) The effect of pressure on deuterium-hydrogen fractionation in high-temperature water. *Science* **277,** 791–794.

Duffy T. S. and Ahrens T. J. (1991) The shock-wave equation of state of brucite $Mg(OH)_2$. *J. Geophys. Res.* **96B,** 14319–14330.

Duffy T. S., Meade C., Fei Y., Mao H-K., and Hemley R. J. (1995) High-pressure phase transition in brucite, $Mg(OH)_2$. *Am. Mineral.* **80,** 222–230.

Frantz J. D., Dubessy J., and Mysen B. (1993) An optical cell for Raman spectroscopic studies of supercritical fluids and its application to the study of water to 500°C and 2000 bar. *Chem. Geol.* **106,** 9–26.

Galimov E. M. (1985) *The Biological Fractionation of Isotopes*. Academic Press, Orlando.

Gillet P., McMillan P., Schott J., Badro J., and Grzechnik A. (1996) Thermodynamic properties and isotopic fractionation of calcite from vibrational spectroscopy of ^{18}O-substituted calcite. *Geochim. Cosmochim. Acta* **60,** 3471–3485.

Guo J. and Qian Y. (1997) Hydrogen isotope fractionation and hydrogen diffusion in the tourmaline-water system. *Geochim. Cosmochim. Acta* **61,** 4679–4688.

Graham C. M., Sheppard S. M. F., and Heaton T. H. E. (1980) Experimental hydrogen isotope studies- I. Systematics of hydrogen isotope fractionation in the systems epidote-H_2O, zoisite-H_2O and AlO(OH)-H_2O. *Geochim. Cosmochim. Acta* **44,** 353–364.

Graham C. M., Harmon R. S., and Sheppard S. M. F. (1984) Experimental hydrogen isotope studies: Hydrogen isotope exchange between amphibole and water. *Am. Mineral.* **69,** 128–138.

Graham C. M., Viglino J. A., and Harmon R. S. (1987) Experimental study of hydrogen-isotope exchange between aluminous chlorite and water and of hydrogen diffusion in chlorite. *Am. Mineral.* **72,** 566–579.

Haar L., Gallagher J. S., Kell G. S. (1984). *NBS/NRC Steam Table.* Taylor & Francis.

Hamann S. D., Shaw R. M., Lusk J., and Batts B. D. (1984) Isotopic volume differences: The possible influence of pressure on the distribution of sulfur isotopes between sulfide minerals. *Aust. J. Chem.* **37,** 1979–1989.

Heybey J. W and U. (1989) Effect of pressure on isotope fractionation in the system CaO-MgO-SiO2-C-H-O. In Proceedings of the 5th Working Meeting Isotopes in Nature, Leipzig, pp. 723– 734.

Hill P. G. (1990) A unified fundamental equation for the thermodynamic properties of H_2O. *Phys. Chem. Ref. Data* **19,** 1233–1274.

Hill P. G., MacMillan R. D. C., and Lee V. (1982) A fundamental equation of state for heavy water. *J. Phys. Chem. Ref. Data* **11,** 1–14.

Hoering T. C. (1961) The physical chemistry of isotopic substances: The effect of physical changes on isotope fractionation. *Carnegie I. Wash.* **60,** 201–204.

Holland T. J. B. and Powell R. (1990) An enlarged and updated internally consistent thermodynamic dataset with uncertainties and correlations—The system K_2O-Na_2O-CaO-MgO-MnO-FeO-Fe_2O_3-Al_2O_3-TiO_2-SiO_2-C-H_2-O_2. *J. Metamorph. Geol.* **8,** 89–124.

Horita J., Wesolowski D. J., and Cole D. R. (1993a) The activity-composition relationship of oxygen and hydrogen isotopes in aqueous salt solutions: I. Vapor-liquid water equilibration of single salt solutions from 50 to 100°C.. *Geochim. Cosmochim. Acta* **57,** 2797–2817.

Horita J., Cole D. R., and Wesolowski D. J. (1993b) The activity-composition relationship of oxygen and hydrogen isotopes in aqueous salt solutions: II. Vapor-liquid water equilibration of mixed salt solutions from 50 to 100°C and geochemical implications.. *Geochim. Cosmochim. Acta* **57,** 4703–4711.

Horita J., Cole D. R., and Wesolowski D. J. (1995) The activity-composition relationship of oxygen and hydrogen isotopes in aqueous salt solutions: III. Vapor-liquid water equilibration of NaCl solutions from to 350°C. *Geochim. Cosmochim. Acta* **59,** 1139–1151.

Horita J., Driesner T., and Cole D. R. (1999) Pressure effect on hydrogen isotope fractionation between brucite and water at elevated temperatures. *Science* **286,** 1545–1547.

Hu G., Clayton R. N. (2002) Oxygen isotope salt effects at high pressure and high temperature, and the calibration of oxygen isotope geothermometers. *Geochim. Cosmochim. Acta* (in press).

Jákli G. and Van Hook W. A. (1981) D/H and $^{18}O/^{16}O$ fractionation factors between vapor and liquid water. *Geochem. J.* **15,** 47–50.

Jancsó G. and Jákli G. (1980) Vapour pressure and ideality of the equimolar mixture of H_2O and D_2O. *Aust. J. Chem.* **33,** 2357–2362.

Jancsó G., Rebelo L. P. N., and Van Hook W. A. (1993) Isotope effects in solution thermodynamics: Excess properties in solutions of isotopomers. *Chem. Rev.* **93,** 2645–2666.

Joy H. W. and Libby W. F. (1960) Size effects among isotopic molecules. *J. Chem. Phys.* **33,** 1276.

Kell G. S. (1977) Effects of isotopic composition, temperature, pressure, and dissolved gases on the density of liquid water. *J. Phys. Chem. Ref. Data* **6,** 1109–1131.

Kestin J., Sengers J. V., Kamgar-Parsi B., and Levelt Sengers J. M. H. (1984a) Thermophysical properties of fluid H_2O. *J. Phys. Chem. Ref. Data* **13,** 175–183.

Kestin J., Sengers J. V., Kamgar-Parsi B., and Levelt Sengers J. M. H. (1984b) Thermophysical properties of fluid D_2O. *J. Phys. Chem. Ref. Data* **13,** 601–609.

Kieffer S. W. (1979) Thermodynamics and lattice vibrations of minerals: 3. Lattice dynamics and an approximation for minerals with application to simple substances and framework silicates. *Rev. Geophys. Space G. E.* **17,** 35–59.

Kieffer S. W. (1980) Thermodynamics and lattice vibrations of minerals: 4. Application to chain and sheet silicates and orthosilicates. *Rev. Geophys. Space G. E.* **18,** 862–886.

Kieffer S. W. (1982) Thermodynamics and lattice vibrations of minerals: 5. Applications to phase equilibria, isotopic fractionation, and high-pressure thermodynamics properties.. *Rev. Geophys. Space G. E.* **20,** 827–849.

Kruger M. B., Williams Q., and Jeanloz R. (1989) Vibrational spectra of $Mg(OH)_2$ and $Ca(OH)_2$ under pressure. *J. Chem. Phys.* **91,** 5910–5915.

Larrieu T. L. and Ayers J. C. (1997) Measurements of the pressure-volume-temperature properties of fluids to 20 kbar and 1000°C: A new approach demonstrated on H_2O. *Geochim. Cosmochim. Acta* **61,** 3121–3134.

Ludwig K. R.(1994) ISOPLOT: A plotting and regression program for radiogenic-isotope data, version 2.71. U. S. G. S. Open-File Report, pp. 91–445.

Matsuhisa Y., Goldsmith J. R., and Clayton R. N. (1979) Oxygen isotopic fractionation in the system quartz-albite-anorthite-water. *Geochim. Cosmochim. Acta* **43,** 1131–1140.

Matthews A., Goldsmith J. R., and Clayton R. N. (1983a) Oxygen isotope fractionations involving pyroxines: The calibration of mineral-pair geothermometers. *Geochim. Cosmochim. Acta* **47,** 631–644.

Matthews A., Goldsmith J. R., and Clayton R. N. (1983b) On the mechanisms and kinetics of oxygen isotope exchange in quartz and feldspars at elevated temperatures and pressures. *Geol. Soc. Am. Bull.* **94,** 396–412.

Mineev S. D. and Grinenko V. A. (1996) The pressure influence on hydrogen isotopes fractionation in the serpentine-water system. *Journal of Conference Abstract* **1,** 404.

Mitra S. S. (1962) Vibration spectra of solids. *Solid State Physics 13* In: (eds. F. Seitz and D. Turnball), pp. 1–80. Academic, New York.

Northrop D. A. and Clayton R. N. (1966) Oxygen-isotope fractionations in systems containing dolomite. *J. Geol.* **74,** 174–196.

Polyakov V. B. (1998) On an harmonic and pressure corrections to the equilibrium isotopic constants for minerals. *Geochim. Cosmochim. Acta* **62,** 3077–3085.

Polyakov V. B. and Kharlashina N. N. (1994) Effect of pressure on equilibrium isotopic fractionation. *Geochim. Cosmochim. Acta* **58,** 4739–4750.

Polyakov V. B. and Kuskov O. L. (1995) A self-consistent model for calculating mineral thermoelastic and caloric parameters. *Geochem. Int.* **32,** 110–138.

Polyakov V. B., Horita J., Cole D. R. Pressure effects on D/H reduced partition functions of water: Evaluation from the equation of state of ordinary and heavy waters. J. Phys. Chem. (in prep.).

Rabinovich I. B. (1970)*Influence of Isotopy on the Physicochemical Properties of Liquids*. Consult Bureau.

Redfern S. A. T. and Wood B. J. (1992) Thermal expansion of brucite, $Mg(OH)_2$. *Am. Mineral.* **77,** 1129–1132.

Richet P., Bottinga Y., and Javoy M. (1977) A review of hydrogen, carbon, nitrogen, oxygen, sulfur, and chlorine stable isotope fractionation among gaseous molecules. *Annu. Rev. Earth Pl. Sc.* **5,** 65–110.

Rosenbaum J. M. (1997) Gaseous, liquid, and supercritical fluid H_2O and CO_2: Oxygen isotope fractionation behavior. *Geochim. Cosmochim. Acta* **61,** 4993–5003.

Saccocia P. J., Seewald J. S., and Shanks III. W. C. (1998) Hydrogen and oxygen isotope fractionation between brucite and aqueous NaCl solutions from 250–450°C. *Geochim. Cosmochim. Acta* **62,** 485–492.

Sakai H. and Tsutsumi M. (1978) D/H fractionation factors between serpentine and water at 100° to 500°C and 2000 bar water pressure, and the D/H ratios of natural serpentines. *Earth Planet. Sci. Lett.* **40,** 231–242.

Satake H. and Matsuo S. (1984) Hydrogen isotopic fractionation factor between brucite and water in the temperature range from 100° to 510°C. *Contrib. Mineral. Petr.* **86,** 19–24.

Saxena S. K. (1989) Assessment of bulk modulus, thermal expansion and heat capacity of minerals. *Geochim. Cosmochim. Acta* **53,** 785–789.

Schmid H., Heybey J., Vörtler H-L. (1989) Influence of composition and state conditions on isotope exchange factor in dense geological systems. In Proceedings of the 5th Working Meeting Isotopes in Nature, Leipzig, pp. 711–721.

Sharp Z. D., Essene E. L., and Smyth J. R. (1992) Ultra-high temperatures from oxygen isotope thermometry for a coesite-sanidine grospydite. *Contrib. Mineral. Petr.* **112,** 358–370.

Suzuoki T. and Epstein S. (1976) Hydrogen isotope fractionation between OH-bearing minerals and water. *Geochim. Cosmochim. Acta* **40,** 1229–1240.

Urey H. C. (1947) The thermodynamic properties of isotopic substances. *J. Chem. Soc.* (London) 562–581.

Varshavsky Y. M. and Vaisberg S. E. (1957) Thermodynamic and kinetic particulars of isotopic exchange reactions. *Usp. Khim.* **26,** 1434–1468 (in Russian).

Vennemann T. W. and O'Neil J. R. (1996) Hydrogen isotope exchange reactions between hydrous minerals and molecular hydrogen: I. A new approach for the determination of hydrogen isotope fractionation at moderate temperatures. *Geochim. Cosmochim. Acta* **60,** 2437–2451.

Vörtler H-L. and Heybey J. (1989) Intermolecular interaction contributions to thermodynamic isotope effects; high density fluid isochors. In Proceedings of the 5th Working Meeting Isotopes in Nature, Leipzig, pp. 699– 710.

Walther J. V. (1986) Experimental determination of portlandite and brucite solubilities in supercritical H_2O. *Geochim. Cosmochim. Acta* **50,** 733–739.

Wenner D. B. and Taylor H. P. Jr. (1973) Oxygen and hydrogen isotope studies of the serpentinization of ultramafic rocks in oceanic environments and continental ophiolite complexes. *Am. J. Sci.* **273,** 207–239.

Withers A. C., Kohn S. C., Brooker R. A., and Wood B. J. (2000) A new method for determining the P-V-T properties of high-density H_2O using NMR: Results at 1.4–4.0 GPa and 700–1100°C. *Geochim. Cosmochim. Acta* **64,** 1051–1057.

Xu B-L. and Zheng Y-F. (1999) Experimental studies of oxygen and hydrogen isotope fractionations between precipitated brucite and water at low temperatures. *Geochim. Cosmochim. Acta* **63,** 2009–2018.

York D. (1969) Least squares fitting of a straight line with correlated errors. *Earth Planet. Sci. Lett.* **5,** 320–324.